

**EFFECT OF CHLOROPHYLL ON P3TAA, PT AND PPY  
THIN FILMS FOR THE FABRICATION OF ORGANIC  
SOLAR CELLS**

**HAMIZAH NADIA BINTI ALIAS @ YUSOF**

**Thesis Submitted in Fulfillment of the  
Requirement for the Degree of Master of Science  
in the School of Fundamental Science  
Universiti Malaysia Terengganu**

**August 2015**

Abstract of thesis presented to the Senate of Universiti Malaysia Terengganu in fulfillment of the requirement for the degree of Master of Science

**EFFECT OF CHLOROPHYLL ON P3TAA, PT AND PPY THIN FILMS FOR THE FABRICATION OF ORGANIC SOLAR CELLS**

**HAMIZAH NADIA BINTI ALIAS @ YUSOF**

**August 2015**

**Main Supervisor : Assoc. Prof. Dr. Mohd Ikmar Nizam Hj. Mohamad Isa, Ph.D**

**Co- Supervisor : Hasiah binti Salleh, M.Sc**

**School : Fundamental Sciences**

In this project, single layer and double layer organic solar cells were fabricated from multi group organic materials; poly (3-thiophene acetic acid) (P3TAA), polythiophene (PT), polypyrrole (PPY) and chlorophyll (CHLO). Single layer thin films were deposited on indium tin oxide (ITO) coated glass substrate by using electrochemical impedance spectroscopy (EIS) and the second layer, CHLO thin film was deposited on top of conjugated polymers thin film by using spin coater, all at room temperature. Electrical properties and optical properties for both types of organic solar cells were studied and determined by four point probe method, two point probe method, both at dark and under different light intensity, and ultraviolet-visible (UV-Vis) spectroscopy respectively. Electrical conductivity for all devices has obviously increased with the existence of CHLO layer and slightly increased with the increasing of light intensity. Among the conjugated polymers, P3TAA thin film with thickness 97.03 nm in average, measured by profilometer, has the lowest energy band gap, 5.6 eV. The decreasing of thin film thickness has increased the energy band gap as a consequence to the amount of photons absorbed. The addition of CHLO thin film for the second layer has enhanced

the performance of devices as well as the power conversion efficiency (PCE). CHLO thin film helps to absorb maximum photons thus decreasing the possibility of charges recombination at donor-acceptor surface. Device with P3TAA thin film has shown the best enhancement in performance with the addition of CHLO layer and its highest PCE is  $10.4 \times 10^{-2}\%$  at  $30 \text{ W/m}^2$  light intensity. The majority charge carrier in all devices was electron, measured by using Hall Effect Measurement (HEM) at room temperature. Consequently, thin film thickness and types of material used did affect the device performance. In principle, organic solar cells can reach an optimum efficiency as inorganic solar cells if the enhancement in design and architecture with the right combination of materials used is found.

Abstrak tesis yang dikemukakan kepada Senat Universiti Malaysia Terengganu sebagai memenuhi keperluan untuk Ijazah Sarjana Sains

**KESAN KLOOROFIL TERHADAP FILEM NIPIS P3TAA, PT DAN PPY UNTUK FABRIKASI SEL SOLAR ORGANIK**

**HAMIZAH NADIA BINTI ALIAS @ YUSOF**

**Ogos 2015**

**Penyelia Utama : Assoc. Prof. Dr. Mohd Ikmar Nizam Hj. Mohamad Isa, Ph.D**

**Penyelia Bersama : Hasiah binti Salleh, M.Sc**

**Pusat Pengajian : Sains Asas**

Untuk projek ini, satu lapisan dan dua lapisan sel solar organik telah dihasilkan daripada campuran kumpulan bahan – bahan organik; poli (3-tiopin asid asetik) (P3TAA), politiopin (PT), polipirol (PPY) dan klorofil (CHLO). Lapisan pertama filem nipis telah disadur di atas permukaan substrat indium tin oksida (ITO) dengan menggunakan alat spektroskopi rintangan elektrokimia (EIS) manakala lapisan kedua, filem nipis CHLO disadur pada permukaan filem nipis polimer dengan menggunakan teknik pemutar bersalut, kedua – duanya pada suhu bilik. Pencirian elektrik dan pencirian optik bagi kedua – dua jenis sel solar organik telah dikaji dan ditentukan dengan menggunakan teknik penduga empat kaki dan penduga dua kaki (dalam keadaan gelap dan keamatan cahaya yang berbeza) dan juga spektroskopi UV-Vis. Kekonduksian elektrik bagi semua alat solat meningkat secara ketara dengan kehadiran lapisan CHLO tetapi hanya meningkat secara sedikit – sedikit apabila keamatan cahaya bertambah. Filem nipis P3TAA dengan purata ketebalan 97.03 nm yang diukur dengan profilometer mempunyai tenaga pemisah terendah iaitu 5.6 eV. Ketebalan filem nipis memberi kesan ke atas bilangan foton yang diserap di mana tenaga pemisah bagi ketebalan filem yang nipis

adalah tinggi, begitu juga dengan sebaliknya. Penyaduran filem nipis CHLO sebagai lapisan kedua telah meningkatkan keupayaan sel solar terutamanya pada nilai kecekapan penukaran tenaga (PCE) sel. Keupayaan filem nipis CHLO untuk menyerap foton pada tahap maksimum dapat mengurangkan kemungkinan bagi cas – cas bebas terikat kembali di kawasan pederma-penerima. Sel solar yang disadur dengan filem nipis P3TAA menunjukkan perubahan prestasi yang mendadak apabila filem nipis CHLO disadur di atasnya hingga menghasilkan nilai PCE yang tertinggi iaitu  $10.4 \times 10^{-2}\%$  pada keamatan cahaya  $30 \text{ W/m}^2$ . Ujian yang dilakukan dengan Pengukuran Kesan Hall (HEM) pada suhu bilik menunjukkan pembawa caj majoriti bagi kesemua sel solar adalah elektron. Melalui projek ini, didapati ketebalan filem nipis dan jenis bahan yang digunakan mempengaruhi keupayaan sel solar untuk menukar cahaya kepada tenaga elektrik. Dalam erti kata lain, sel solar organik mampu untuk menghasilkan nilai PCE yang tinggi seperti sel solar tak organik sekiranya dapat mencapai rekabentuk dan susun atur serta kombinasi bahan yang digunakan dengan tepat.

## ACKNOWLEDGEMENT

First of all, praise to Allah s.w.t for giving me strength and passion to complete this thesis for my degree of master. Alhamdulillah.

First and foremost, I would like to express my appreciation and gratitude to my supervisor, Assoc. Prof. Dr. Mohd Ikmar Nizam Hj. Mohamad Isa and my co-supervisor, Puan Hasiah Bt. Salleh for their supervisions, invaluable advices, encouragement and continuous guidance throughout the course of this project. Especially I feel thankful to Puan Hasiah for believing in me and giving me this precious opportunity to further my study under her supervision. She is certainly the person who gives me a lot of constructive comments and ideas for this successful completion project. Thank you for being patient with me all the times.

Next, I would like to acknowledge the Ministry of Higher Education for financially support this project through FRGS Grant vot 55065. I would like to thank lab staffs at Physical Sciences Department in Universiti Malaysia Terengganu and Universiti Kebangsaan Malaysia for the technical equipments. Not to forget my appreciation to Master's students, En. Nik Aziz bin Nik Ali and Puan Norlaily bt. Abdul Rashid for their guidance and knowledge in helping me complete this project. A big contribution and hard work from all of them during the project is very great indeed.

Besides that, I would like to utter my deeply and warmest thankful to my family members especially to my beloved parents for their love, support and encouragement through physical, mental and financial. My thankful also intended to my lab partners, Wan Almaz Dafina and Fardiana for always being there for me in helping and guiding me to solve problems related to this project.

Last but not least, a genuine thank you for those who involved directly or indirectly in this project, your kindness and co-operation are appreciated. May Allah bless all of you. Thank you.

## APPROVAL

I certify that an Examination Committee has met on 2<sup>nd</sup> August 2015 to conduct the final examination of Hamizah Nadia binti Alias @ Yusof on her Master of Science thesis entitled “Effect of Chlorophyll on P3TAA, PT and PPY Thin Films for the Fabrication of Organic Solar Cells” in accordance with the regulations approved by the Senate of Universiti Malaysia Terengganu. The Committee recommends that the candidate be awarded the relevant degree. The members of the Examination Committee are as follows:

Wan Mohd Khairul bin Wan Mohamed Zain, Ph.D.  
Associate Professor  
School of Fundamental Science  
Universiti Malaysia Terengganu  
(Chairperson)

Chan Kok Sheng, Ph.D.  
Lecturer  
School of Fundamental Science  
Universiti Malaysia Terengganu  
(Internal Examiner)

Azwani Sofia binti Ahmad Khair, Ph.D.  
Associate Professor  
Faculty of Science and Technology  
Universiti Sains Islam Malaysia  
(External Examiner)

---

**NAKISAH BINTI MAT AMIN, Ph.D.**  
Professor/Dean of School of  
Fundamental Science,  
Universiti Malaysia Terengganu

Date:

This thesis has been accepted by the Senate of Universiti Malaysia Terengganu as fulfillment of the requirements for the degree of Master of Science.

---

**NAKISAH BINTI MAT AMIN, Ph.D.**  
Professor/Dean of School of  
Fundamental Science,  
Universiti Malaysia Terengganu

Date:



## DECLARATION

I hereby declare that the thesis is based in my original work except for quotations and citations which have been duly acknowledged. I also declare that it has not been previously or concurrently submitted for any other degree at UMT or other institutions.

---

HAMIZAH NADIA BINTI ALIAS @ YUSOF

Date:

## TABLE OF CONTENTS

	<b>Page</b>
ABSTRACT	ii
ABSTRAK	iv
ACKNOWLEDGEMENT	vi
APPROVAL	vii
DECLARATION	ix
TABLE OF CONTENTS	x
LIST OF TABLES	xii
LIST OF FIGURES	xiii
LIST OF ABBREVIATIONS	xv
<b>CHAPTER</b>	
<b>1 INTRODUCTION</b>	
1.1 Background of the Study	1
1.2 Statement of the Problem	3
1.3 Significance of the Study	4
1.4 Scope of the Study	4
1.5 Objectives of the Study	5
1.6 Thesis Organization	6
<b>2 LITERATURE REVIEW</b>	
2.1 Organic Solar Cell	7
2.2 Organic Semiconductor	14
2.3 Conjugated Polymers	17
2.3.1 Polypyrrole	19
2.3.2 Polythiophene	20
2.3.3 Poly (3-thiophene acetic acid)	23
2.4 Chlorophyll	25
<b>3 METHODOLOGY</b>	
3.1 Sample Preparation	
3.1.1 Cleaning ITO slides	28
3.1.2 Etching ITO layer on glass substrate	29
3.1.3 Single layer thin film deposition	30
3.1.4 Coating chlorophyll thin film	32
3.2 Sample Characterization	
3.2.1 Thickness measurement	34
3.2.2 Energy band gap measurement	35
3.2.3 Electrical conductivity measurement	36
3.2.4 Power conversion efficiency measurement	37
3.2.5 Hall Effect measurement (HEM)	39

<b>4</b>	<b>RESULTS AND DISCUSSION</b>	
4.1	Thickness Measurement	43
4.2	Energy Band Gap Measurement	45
4.3	Electrical Conductivity Measurement	51
4.4	Hall Effect Measurement	54
4.5	Power Conversion Efficiency	60
<b>5</b>	<b>GENERAL DISCUSSION</b>	
5.1	Discussion	66
<b>6</b>	<b>CONCLUSION AND RECOMMENDATION</b>	
6.1	Conclusion	72
6.2	Recommendation	73
	REFERENCES	74
	APPENDICES	84
	BIODATA OF AUTHOR	94

## LIST OF TABLES

Table No.		Page
2.1	Organic solar cells parameters of the cells fabricated with polymer dyes (Yanagida <i>et al.</i> , 2004).	24
3.1	Procedure set for cyclic voltammetry (staircase) method.	32
3.2	Input parameters for IV curve traces.	41
3.3	Input parameters for variable magnetic field measurement.	41
4.1	Thickness of polymers thin film and chlorophyll thin film deposited on ITO coated glass substrate.	44
4.2	Efficiency and other parameters for all devices before and after depositing CHLO thin film under 100 W/m <sup>2</sup> intensity.	62
4.3	Percentage difference of efficiency values of organic solar cells before and after CHLO thin film deposition at various light intensities.	64

## LIST OF FIGURES

Figure No.		Page
2.1	Illustration showing current generation mechanism in OPV (Kim, 2009).	8
2.2	Illustration schematic of single layer OPV (Kim, 2009).	9
2.3	Schematic illustration of a double layer OPV (a), a bulk heterojunction OPV (b) and an ordered bulk heterojunction OPV (c) (Boudouris, 2009).	10
2.4	Typical current-voltage curve for a photovoltaic cell under dark (black) and under illumination (orange) (Boudouris, 2009).	12
2.5	Solar spectra for AM0 and AM1.5 air mass condition. (Kim, 2009).	16
2.6	Monomer repeat unit of Polypyrrole (Chen, 2007).	20
2.7	The monomer repeat unit of PT (Chen, 2007).	21
2.8	Chemical structure of P3SHT. Due to the extra carboxylate group on the side chain this polythiophene dissolves in water (Haeldermans <i>et al.</i> , 2008).	22
2.9	Monomer repeat unit of P3TAA (Yanagida <i>et al.</i> , 2004).	23
2.10	Structure of CHLO a (a) and CHLO b (b) (Kashiyama <i>et al.</i> , 2013).	25
2.11	Absorbance spectra of CHLO a and CHLO b (Sun & Wang, 2004).	26
3.1	Illustration of ITO layer etching process.	30
3.2	Illustration of electrochemical cell under three electrode configuration (b).	31
3.3	Illustration of organic solar cell.	33
3.4	Schematic diagram of of 4200-SCS's SMU to solar cell connection.	38
3.5	Sample holder with mounted substrate and leads.	39
3.6	Flowchart of methodology.	42
4.1	Energy band gap of P3TAA single layer thin film (a) and energy band gap of P3TAA/CHLO layer by layer thin film (b) on Quartz slides.	46
4.2	Energy band gap of PPY single layer thin film (a) and energy band gap of PPY/CHLO layer by layer thin films (b) on Quartz slides.	47
4.3	Energy band gap of PT single layer thin film (a) and energy band gap of PT/CHLO layer by layer thin films (b) on Quartz slides.	48
4.4	Energy band gap of single layer CHLO thin film deposited on Quartz slide.	49

<b>4.5</b>	Illustration of energy required by electron to be excited from HOMO to LUMO level before coating CHLO layer (a) and after coating CHLO layer (b).	50
<b>4.6</b>	The dependence of electrical conductivity on light intensity of single layer thin films deposited on ITO coated substrates.	51
<b>4.7</b>	Comparison of electrical conductivity polymers thin film before and after CHLO thin film deposition.	53
<b>4.8</b>	Hall voltage of organic solar cells without and with the existence of CHLO thin film at 1 Tesla applied magnetic field.	55
<b>4.9</b>	Hall coefficient of organic solar cells without and with CHLO thin film deposition at 1 Tesla applied magnetic field.	56
<b>4.10</b>	Carrier concentration of organic solar cells without and with CHLO thin film deposition at 1 Tesla applied magnetic field.	57
<b>4.11</b>	Hall mobility of organic solar cells without and with the existence of CHLO thin film deposition at 1 Tesla applied magnetic field.	59
<b>4.12</b>	ITO substrate without any deposition (a), ITO substrate with polymer and CHLO deposition (b) and complete organic solar cell with Aluminium electrode deposition (c).	61
<b>4.13</b>	J-V characteristic of organic solar cell in dark and under illuminate condition.	62
<b>4.14</b>	Efficiency (in percentage) of organic solar cells before (solid bar) and after deposited with CHLO thin film (lined bar) at intensity $100 \text{ W/m}^2$ .	64

## LIST OF ABBREVIATIONS

### Abbreviations

$\pi$	Pi
$\sigma$	Conductivity
$\eta$	Efficiency
$\eta_{EQE}$	External quantum efficiency
$\mu$	Mobility
$\mu_H$	Hall mobility
$\tau$	Lifetime of bulk materials
$\lambda$	Wavelength
$^{\circ}\text{C}$	Degree Celsius
%	Percentage
Ag	Silver
AgCl	Silver chloride
Al	Aluminium
BCP	Bathocuproine
$B_z$	Magnetic field in z-axis
$c$	Speed of light
$\text{C}_{60}$	Fullerene
Ca	Calcium
CE	Counter electrode
$\text{CHCl}_3$	Chloroform
$\text{CO}_2$	Carbon dioxide
DMF	Dimethylformamide
DSSC	Dye-sensitized solar cells
$e$	Charge of electron
$E_g$	Energy band gap
EIS	Electrochemical Impedance Spectroscopy
eV	Electron volt
FF	Fill factor
GPES	General purpose electrochemical system
$h$	Planck's constant
HCl	Hydrochloric
HEM	Hall Effect measurement
HOMO	Highest Occupied Molecular Orbital
$I$	Current
$I_o$	Initial current
$I_m$	Maximum current
$I_{SC}$	Short circuit current
ITO	Indium Tin Oxide
I-V	Current-voltage characteristic
$I_x$	Current in x-axis
$J_{SC}$	Short circuit photocurrent

J-V	Current density-voltage characteristic
$k$	Boltzmann constant
kG	Kilogauss
kHz	Kilohertz
LUMO	Lowest Unoccupied Molecular Orbital
$M$	Reducing agents
Mg	Magnesium
MHImI	1-methyl-3-n-hexylimidazolium iodide
ml	milliliter
NH <sub>4</sub> OH	Ammonium dioxide
$n$	Carrier concentration
nm	nanometer
$n$ -doping	Reduction reaction (electron-donating)
$n$ -type	negative-type (donor)
OLED	Organic light-emitting diode
OPV	Organic Photovoltaic
OSC	Organic Solar Cells
$p$ -doping	Oxidation reaction (electron-accepting)
$p$ -type	positive-type (acceptor)
P3HT	Poly(3-hexyl thiophene)
P3SHT	Poly[3-(sodium-6-hexanoate)thiophene-2,5-diyl]
P3TAA	Poly(3-thiophene acetic acid)
P3TAA-PHT	Poly(3-thiophene acetic acid)-poly(hexyl thiophene)
PCE	Power conversion efficiency
PGSTAT	Potentiostat/galvanostat
pH	Power of hydrogen
$P_{in}$	Input power
$P_m$	Maximum power
PPV	Poly(p-phenylene vinylene)
PPY	Polypyrrole
PT	Polythiophene
PTCBI	perylene-3,4,9,10-bis-benzimidazole
PVD	Physical vapour deposition
$q$	Elementary charge
RE	Reference electrode
$R_{H\ avg}$	The average of Hall coefficient
$R_{HC}$	Hall coefficient in vertical
$R_{HD}$	Hall coefficient in horizontal
rpm	Rotation per minute
$R_s$	Serial resistance
$R_{sh}$	Shunt resistance
$R_{st}$	Sheet resistivity
SCS	Semiconductor characterization system
SMU	Source measure unit
$t$	Film thickness
$T$	Temperature



TiO <sub>2</sub>	Titanium dioxide
TPP	Two point probe method
UKM	Universiti Kebangsaan Malaysia
UV-Vis	Ultraviolet-Visible
V	Voltage
vdP	van der Pauw
$V_H$	Hall voltage
$V_{H\ avg}$	The average of Hall voltage
$V_{H\ total}$	Total of Hall voltage
$V_m$	Maximum voltage
$V_{OC}$	Open circuit voltage
WE	Working electrode
X	Oxidizing agents

## CHAPTER 1

### INTRODUCTION

#### 1.1 Background of the Study

Fossil fuels, renewable resources and nuclear resources are three categories for energy resources classification (Demirbas, 2000). Among those three categories, fossil fuels have been the dominant energy source including oil, coal and natural gas. Currently, the industrial sector consumes about 37% of the world's total delivered energy, the highest energy usage compared to any other end-use sectors as stated in the report by Abdelaziz *et al.* (2011). The reserves of fossil fuels are lessening since their formation through natural process could take thousands and up to millions of years and their large-scale use is associated with environmental deterioration (Manzano, 2010 and Manzano *et al.*, 2012). According to Kalogirou (2004), acid precipitation, stratospheric ozone depletion and the global climate change are three major international environmental problems.

The increasing of fuel prices along with the excessive carbon dioxide (CO<sub>2</sub>) emissions are the urgent motivations for researches to harvest in both energy saving strategy and

renewable energy resources utilization (Banos *et al.*, 2011 and Panwar *et al.*, 2011). Dincer (1999) and Charters (2001) have defined renewable energy resources as sustainable resources available over the long term and not exhaustible by its use in producing electricity or heat (steam) or mechanical energy without generating negative effects. These resources include biomass, hydropower, geothermal, solar, wind and marine energies. However, Lenzen (2010) has reported that the recent annual growth rates of about 40% for solar and 34% for wind powers are probably the strongest-growing electricity generating technologies. Last year, as reported by Manzano *et al.* (2013), the total world energy production for renewable energy sources is about 14% and expected to increase significantly until the end of century.

Over these decades, solar cells have increasing interest among researches as a replacement to the dominant energy source. The inorganic solar cells are able to contribute higher power conversion efficiency and last long in lifetime. However the high cost in fabricating inorganic solar cells has lead researches to pay extreme attention to fabricate organic solar cells with much lower production cost. There are three major types of solar cells; single layer, planar heterojunction and bulk heterojunction. In order to increase and optimize the cells performance, the solar cells structure is tailored in various ways. The tandem cells (combination of multiple layers) and well ordered bulk heterojunction cells have been widely manufactured nowadays. Many studies have used organic polymers or conjugated polymers as an active layer in solar cells for their remarkable advantages especially the ability to conduct electric. However the individual characteristic and the consequence towards device performance as an active layer have become our focus in this project.

## 1.2 Statement of the Problem

Many group studies have fabricated organic solar cells from conjugated polymers such as polythiophene (PT) and polypyrrole (PPY) for their lower cost production. However organic solar cell fabrication by using poly (3-thiophene acetic acid) (P3TAA) thin film as an active layer has not yet been studied widely. This project is focusing on the characteristics of PT, PPY and P3TAA thin film as an active layer in both single layer and multi layer organic solar cell arrangement (combine with chlorophyll thin film). Since conjugated polymers absorb spectrum at lower wavelength, around 250 nm to 300 nm, this limits the amount of photons absorbed into cells. Chlorophyll (CHLO) thin film, a material that could absorb spectrum in wide range, will be used by coating it on an organic compound to increase the amount of absorbed light to be converted into electricity thus automatically increasing the efficiency of devices. The thickness of single layer conjugated polymer thin film will be determined to investigate its consequences toward device performance. Electrical properties and optical properties comparison between these three conjugated polymers as an active layer in organic solar cell will be studied to observe factors affecting device parameters, power conversion efficiency and performances. Both electrical and optical properties will be characterized under dark condition and under various light intensities. Hall voltage and Hall coefficient for each device will also be measured to determine the majority type of charge carrier.

### **1.3 Significance of the Study**

This study provides more knowledge on the fabrication of single layer and multi layer thin film(s) from multi organic materials as organic solar cells. It also presents knowledge on the effect of CHLO thin film toward organic solar cells performance. Besides that this study may also offer the best arrangement of organic thin films to produce a higher power conversion efficiency cell. Electrical and optical properties of single layer conjugated polymer thin film and the combination with CHLO thin film under various light intensities are also presented. In fact, Hall effect measurement on single layer and double layer organic solar cell and the type of charge carriers are also provided in this study. Further understanding on the fabrication and characterization could venture emerging and potentially transformative research ideas. Overall this study will significantly increase the knowledge of organic solar cell since it is a preliminary work. In order to complete the research, there are main objectives targeted in this study.

### **1.4 Scope of the Study**

In this study, P3TAA, PPY, PT and CHLO thin films are fabricated on ITO glass substrate separately by using EIS at room temperature. CHLO thin film is deposited on top of P3TAA, PPY and PT thin film as second layer by using spin coater at room temperature.

The thickness of single layer thin film will be measured by using profilometer. UV-Vis spectrometer will be used to measure the energy band gap of single layer and double layer thin films. Electrical conductivity of thin films is characterized by using four point

probe method in dark condition and under five different light intensities ( $20\text{W}/\text{m}^2$ ,  $40\text{W}/\text{m}^2$ ,  $60\text{W}/\text{m}^2$ ,  $80\text{W}/\text{m}^2$  and  $100\text{W}/\text{m}^2$ ). Hence the effect of light intensity on thin films conductivity can be studied.

The Hall Effect Measurement System is used to determine the Hall voltage, Hall coefficient, carrier concentration and Hall mobility of polymer thin films before and after depositing CHLO layer. Besides, type of charge carrier in thin films can also be determined.

The PCE of single layer and double layer organic solar cells will be calculated by using two point probe method at room temperature in dark condition and under various light intensities ( $10\text{W}/\text{m}^2$ ,  $30\text{W}/\text{m}^2$ ,  $60\text{W}/\text{m}^2$  and  $100\text{W}/\text{m}^2$ ). The effect of light intensity on cells performance can be observed.

## **1.5 Objectives of the Study**

The aims of the study are:

- i. To deposit PPY, PT, P3TAA and CHLO thin film on ITO substrate and measure the thickness of film as an active layer in organic solar cell.
- ii. To determine the energy band gap and electrical conductivity of PPY, PT, P3TAA and CHLO as single layer thin film and the addition of CHLO layer on top of conjugated polymers as double layer thin films in dark and under different light intensities.

- iii. To examine the performance of single layer and double layer organic solar cells by determining the type of charge carriers and by measuring the fill factor, short circuit current, open circuit voltage and the power conversion efficiency.

## **1.6 Thesis Organization**

This thesis is composed into five chapters. The first chapter states the background of the research, statement of the problem, significance of study and the research objectives. The second chapter provides literature reviews related to this project that are done by other researches. The main topics are Organic Solar Cells, Organic Semiconductor, Conjugated Polymer (PPY, PT and P3TAA), and Chlorophyll (CHLO).

The third chapter explains the methodology including details on the instruments used for preparation and characterizing samples. The instruments include ultrasonic bath, Electrochemical Impedance Spectroscopy (EIS), spin coater, profilometer, ultraviolet-visible (UV-Vis) spectroscopy, four point probe, two point probe and Hall effect measurement system. The fourth chapter shows results that are gathered through this research in various form such as tables and graphs followed by evaluations and discussions. Lastly, the fifth chapter concludes this research in overall based on results and discussions provided along with the objectives stated in first chapter. Besides, recommendations for further research are also included in this final chapter.

## CHAPTER 2

### LITERATURE REVIEW

This chapter contains basic knowledge on organic solar cell, important parameters in determining cell's performance, organic semiconductor and conjugated polymer including information about all four materials used in this study which are PT, PPY, P3TAA and CHLO.

#### 2.1 Organic Solar Cell

Solar cell is an environmentally friendly energy source that converts light absorbed from the sun to electricity (Janssen, 2005). Organic solar cells (OSC) will soon be able to replace inorganic systems if and only if marketing demands such as power efficiency (~10%) and lifetime device (~10 years) can be achieved on a large scale. Since individual characteristic of organic semiconductor differ to inorganic material, the mechanism device operation itself is also different. In organic photovoltaic (OPV) cells, the process of converting light to electricity is composed of five general steps; (a) light absorption, (b) exciton formation, (c) exciton diffusion, (d) exciton separation, and (e) charge transport and collection. A schematic representation of the steps is shown in Figure 2.1.



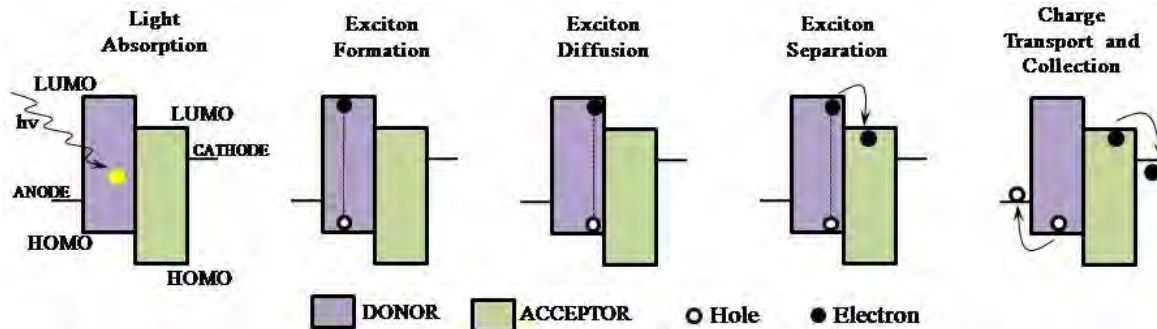


Figure 2.1: Illustration showing current generation mechanism in OPV (Kim, 2009).

Rather than conduction and valence band, the designated state for hole and electron transport are referred to as Highest Occupied Molecular Orbital (HOMO) and Lowest Unoccupied Molecular Orbital (LUMO). As in single layer OSC, the organic semiconductor layer is sandwiched between transparent electrode (high work function) and opaque electrode (low work function) like the one that had been fabricated by Chamberlain (1983) and Wöhrlé *et al.* (1991) in the early generation. Typically indium tin oxide (ITO) layer acts as anode and metal such as Ag, Al, Mg or Ca acts as cathode, as illustrated in Figure 2.2. The device mechanism is quite different compared to double layer and bulk heterojunction OSC since donor-acceptor interface, where exciton diffusion and separation take place, does not exist. As light is absorbed by organic layer, electron is excited to LUMO and leaves hole in HOMO. A pair of electron and hole is Coulombically bound and exciton formation occurs. The built-in electric field in organic layer is created due to the difference in work function between those two electrodes. In fact, this field helps to separate exciton pair by pulling electron to cathode and hole to anode (Kaur *et al.*, 2014).

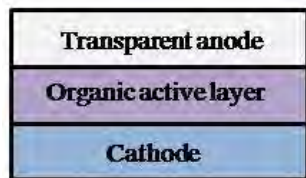


Figure 2.2: Illustration schematic of single layer OPV (Kim, 2009).

Antoniadis *et al.* (1994) had fabricated single layer ITO/PPV/Al device with poly(p-phenylene vinylene) as an active layer and ITO and aluminium (Al) were used as anode and cathode respectively. Only 0.07% of power conversion efficiency (PCE) had been determined. Later, Rieß *et al.* (1994) had fabricated the same structure of device with typical values of open circuit voltage,  $V_{OC}$  range between 0.7 V to 1.3 V. It was reported that short circuit,  $I_{SC}$  was approximately proportional to the light intensity and  $V_{oc}$  varies logarithmically, as expected for Schottky diode. Value for fill factor (FF) varied from 0.2 to 0.3 and PCE was off the order of 0.1% to 1% (calculation including reflection losses). Another research done by Marks *et al.* (1994) had reported a better device performance with quantum efficiency 0.1% under  $0.1 \text{ mW/cm}^2$  intensity. The thickness of an active layer were varied between 50 nm to 320 nm and sandwiched between ITO electrode and a low work function cathode. In order to overcome exciton-binding energy and to separate Coulomb interacting bounded electron-hole pairs, an applied field of more than  $10^6 \text{ Vcm}^{-1}$  is required for exciton dissociation in single organic material.

As for double layer and bulk heterojunction OSC, two different organic materials that act as electron donor and electron acceptor respectively, are sandwiched between electrodes. The electron acceptor has higher electron affinity and ionization energy than that of electron donor (Yeh and Yeh, 2013). However device structure for both types is

different as well as shown in Figure 2.3, where double layer cells are fabricated by depositing materials layer by layer and bulk heterojunction cells are manufactured by blending two materials together. Once an exciton is formed and diffused to donor-acceptor interface, material with lower ionization energy accepts hole and material with higher electron affinity accepts electron (Brabec *et al.*, 2001). Grossiord *et al.* (2012) has mentioned that the dissimilarity in characteristic is more efficient to trigger exciton dissociation compared to single layer cells.

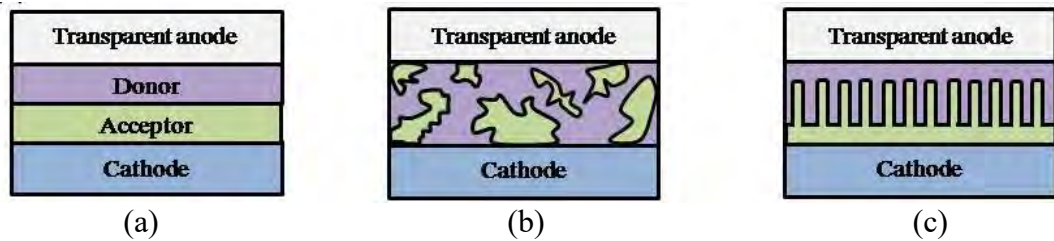


Figure 2.3: Schematic illustration of a double layer OPV (a), a bulk heterojunction OPV (b) and an ordered bulk heterojunction OPV (c) (Boudouris, 2009).

Since high applied fields are required to overcome exciton-binding energy and to separate Coulomb interacting bounded electron-hole pairs, it is impossible for a typical operation of OSC to generate such strong electric field by voltages (Mishra and Buerle, 2012). In fact, the recombination losses in single layer OSCs are extremely high and led to a low efficiency. This is because the positive and negative photoexcited charges have to travel through the same material to reach their appropriate electrodes. However, Tang (1986) had overcome these disadvantages by developing bilayer planar heterojunction using Cu-phthalocyanine as the donor layer and perylene-3,4,9,10-bis-benzimidazole (PTCBI) as the acceptor layer with thickness of 30 nm and 50 nm respectively. These materials were sandwiched between transparent ITO electrode (anode) and silver electrode (cathode). It was reported that even at  $75 \text{ mWcm}^{-2}$  light intensity, the PCE was

increased up to 0.95% with an impressive fill factor (FF) of 65%. Charges diffusion and charge dissociation are attributed to the difference in energy level of LUMO and HOMO of donor and acceptor layers. The enhancement of devices structure was later becoming major interest among researches to fabricate higher efficiency organic photovoltaic cells. This includes the one called tandem cell, where two separate multilayer cells are sandwiched or combined together as one device.

The external quantum efficiency ( $\eta_{EQE}$ ), which is defined as the number of electrons produced by a PV cell for each photon absorbed is ultimately limited by the number of photons absorbed by photoactive layer within an exciton diffusion length. However in organic materials, the diffusion length of an exciton is generally short and limited to about 5 nm – 20 nm (Halls *et al.*, 1996 and Savanije *et al.*, 1998) and become a disadvantage for an optimum exciton diffusion to occur during its lifetime (Pettersson *et al.*, 1999, Haugeneder *et al.*, 1999 and Stoessel *et al.*, 2000). If an exciton does not dissociate completely into free charge carrier, it either eventually recombines by emitting a photon or decaying via thermalization (Hoppe *et al.*, 2008). Once the charge carriers are successfully separated, electrons and holes are transported to and collected at their respective electrodes and passed into the outer circuit to generate device photocurrent. As reported by Mihailetchi *et al.* (2004) and Hwang *et al.* (2009), the charge collection efficiency not only depends on the energy level matching at metal/polymer interface but also depends on the interfacial defects.

Solar cells with optimum performance are the one that have higher PCE where the value strictly depends on the device parameters. Higher efficiency means that solar cells are able to convert a maximum absorbed light into electrical energy. These parameters are determined and calculated through current-voltage (I-V) curve characteristic. The typical I-V curve for photovoltaics in Figure 2.4 shows both in the dark and under illumination.

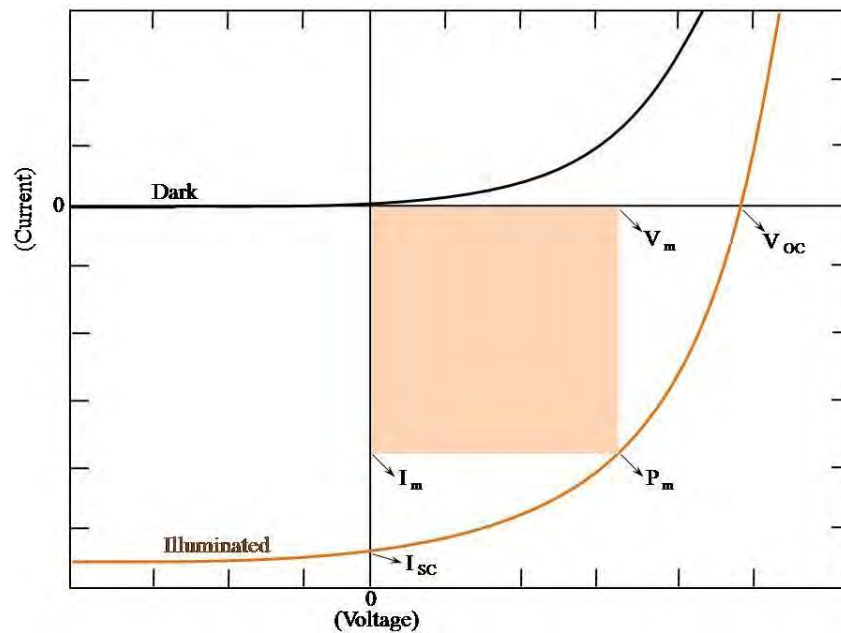


Figure 2.4: Typical current-voltage curve for a photovoltaic cell under dark (black) and under illumination (orange) (Boudouris, 2009).

Current under dark condition follows the form of the Shockley equation for an ideal diode.

$$I = I_o \left( e^{qV/kT} - 1 \right) \quad (2.1)$$

Here,  $q$  is the elementary charge,  $k$  is Boltzmann constant,  $V$  is voltage across the diode, and  $T$  is the temperature. Under illumination, even without any external applied voltage,

a photocurrent occurs and determines the value of short circuit current,  $I_{SC}$ . Photocurrent is actually a reverse bias current since electrons flow toward cathode and holes flow toward anode. After applying voltage, a forward bias current occurs and will start compensating for that reverse photocurrent until reaching at one point where current goes zero. This point refers to open circuit voltage,  $V_{OC}$  where the system is assumed to be opened because no current flow in the circuit even with an applied voltage. FF delineates the quality of the curve in the 4<sup>th</sup> quadrant and is more sensitive parameter in comparison to  $I_{SC}$  and  $V_{OC}$ . FF is not only dependent on the mobility ( $\mu$ )–lifetime ( $\tau$ ) product of the bulk materials, but also on thickness of the active layer and the morphology of interface between cathode/active layer (Gupta *et al.*, 2010). The relation between FF, current and voltage is shown in Equation 2.2.

$$FF = \frac{(I_m)(V_m)}{(I_{SC})(V_{OC})} \quad (2.2)$$

Additionally, FF is mostly influenced by two extrinsic factors; (1) the shunt resistant ( $R_{sh}$ ) which generally reflects the degree of leakage current through the whole device and often linked to imperfections during the production process, and (2) the serial resistant ( $R_s$ ) which is particularly due to the resistivity of all materials of the OPV stack, the resistivity of the metallization, as well as by the contact resistance between various materials especially at the photoactive layer/electrode interface (Grossiord *et al.*, 2012). One of the square-area's edges that lie along the curve in the 4<sup>th</sup> quadrant is referred to as maximum power,  $P_m$  of the device. Maximum power,  $P_m$  is the product of maximum current,  $I_m$  to maximum voltage,  $V_m$ . Once the input power,  $P_{in}$  is known, the PCE of the device can be calculated with given formula.

$$\text{PCE} = \frac{(I_{SC})(V_{OC})(FF)}{P_{in}} \quad (2.3)$$

Input power,  $P_{in}$  is the product of light intensity ( $\text{Wm}^{-2}$ ) to the surface area of the device ( $\text{m}^2$ ). In other word, PCE of a solar cell is the percentage of light absorbed that is converted into power electric. The intensity of light projected on device plays a big role in determining power conversion efficiency, PCE. As light intensity decreasing, only a small amount of light absorbed into device and not sufficient enough to be converted into high electricity. Recombination of free charges at the interface of active layer and acceptor layer contribute to the efficiency reduction. This reduction occurs as free charges fail to be transported to the appropriate electrode before converting into electricity. As higher light intensity projected onto solar device, more amount of light are absorbed into thus reducing the chance for free charges to recombine in the active layer and optimizing the performance of solar device. This circumstance has already been proven by a group of researches (Zhang *et al.*, 2010; Steima *et al.*, 2011; Liu & Liu, Valls *et al.*, 2011; Wehenkel *et al.*, 2012). OSCs which made up of organic semiconductor as an active layer offer many advantages in various organic electronic applications such as organic solar cell, organic light emitted diode and organic gas sensor.

## 2.2 Organic Semiconductor

In organic semiconductors, the intermolecular interactions are much weaker since the organic molecular crystals are van-der-Waals-bonded as compared to covalently bonded in inorganic semiconductors and this condition prevent the formation of band-like

transportation (Sun and Sariciftci, 2005). Hagen (2006) had stated that carbon-carbon bonds in organic semiconductors molecules alternate single and double bonds, meaning that there are only three atoms covalently bonded to each  $sp^2$ -hybridized carbon nucleus. This hybridization significantly allows valence p-orbital electrons to become delocalized and contribute to current. Organic semiconductors can either be  $p$ -type or  $n$ -type materials. Due to instability of organic carbanions to water and oxygen as stated by Dimitrakopoulos *et al.* (2002) and Newman *et al.* (2004), there are more electron donors than that of electron acceptors, so they are commonly classified as  $p$ -type materials.

According to Farchioni and Grosso (2001), there are two major classes of organic semiconductors: small molecules and polymers. Each class has its own advantages and limitations. However, the most important difference between them is the formation of thin films. Small molecules thin films are usually deposited by the gas phase either by sublimation or thermal evaporation (since they are not soluble in common organic solvents) but organic polymers thin films are deposited by solution either by spin coating or printing technique or electrochemical cell. Additionally, a number of low-molecular weight materials (small molecules) can be grown as single crystals or desired films with a relatively high degree of crystallinity if molecules are well-characterized and the deposition technique is well-controlled (de Boer *et al.*, 2004 and Tang *et al.*, 2008). For marketing benefits, industrial sector tend to produce low-cost fabrication products. Since thermal deposition is thought to be more costly than solution process, high efficiency device fabrication using organic polymer has become the prior attention for researches (Boudouris, 2009).



Organic semiconductors can absorb a significant fraction of incident sunlight. Even in thin film (around 100 nm to 500 nm thick), they can absorb light at their peak absorption wavelength as compared to inorganic semiconductors such as crystalline silicon film (around 100  $\mu\text{m}$  thick). Figure 2.5 shows the solar spectrum for both at AM0 (for space application) and AM1.5 (illumination for solar cell performance characterization in terrestrial application). Since the AM1.5 solar spectrum defines a precise spectrum, Rostalski & Meissner (2000) recommended utilizing this spectrum in determining PCE of organic semiconductor based devices. However, organic semiconductors cannot absorb light with longer wavelength due to their relatively large band gap and narrow bandwidth absorption. Therefore, researches are actively paying more attention in finding low band gap organic semiconductors ( $E_g < 1.5$  eV) for a maximum light absorption to occur (Roncali, 1997).

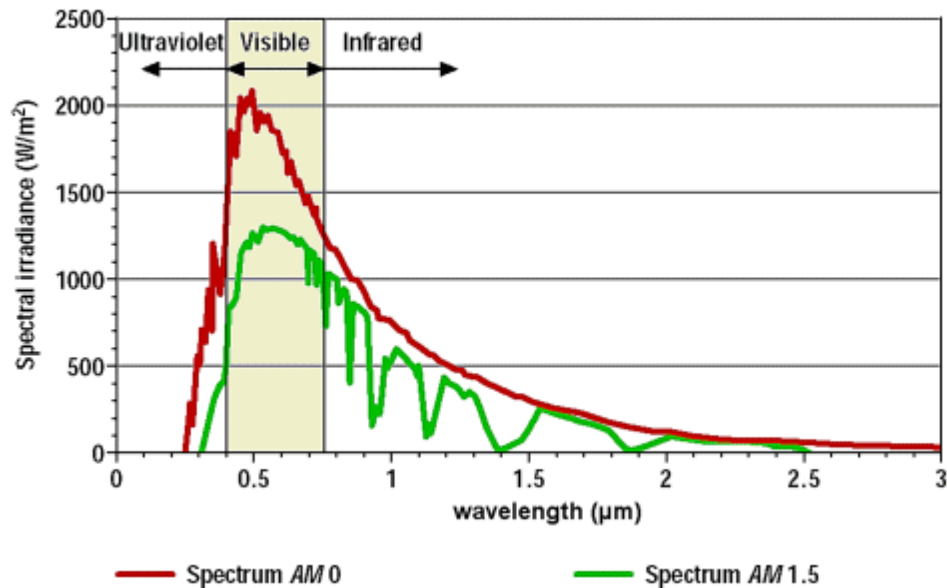


Figure 2.5: Solar spectra for AM0 and AM1.5 air mass condition (Kim, 2009).

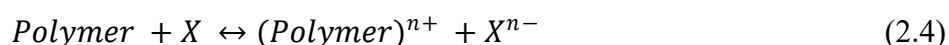
As mentioned before, organic polymers can be casted from solution using wet-processing techniques due to side chains attachment that make them soluble in common organic solvents. These techniques can be performed at ambient temperature and pressure. In addition, solubility of organic polymer make it easy to produce its solvent and also affect the microscopic morphology of thin film formed during solution processing. Another advantage of this polymer is that their molecular weight can be tailored as desired and the optoelectronic properties can be easily tuned by manipulating their chemical structure. Even with little material, an inexpensive large-scale device with good performance for various domestic applications can be fabricated (Pagliaro *et al*, 2008) if a better understanding of conjugated polymers characteristic was achieved.

### **2.3 Conjugated Polymers**

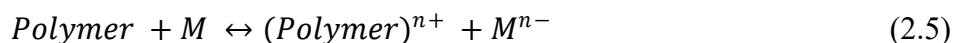
The „conjugate“ from the Latin word „conjugatus“ means to join or unite. William (2005) defines conjugated polymer as a carbon-based macromolecule through which the valence  $\pi$ -electrons are delocalized. In other word these electrons are not associated with a particular atom or bond in that molecule and can only move to a carbon with  $sp^2$  hybridization and not to  $sp^3$  carbon. This is because  $sp^3$  carbon already have full octet and cannot accommodate any more electrons but vice versa for  $sp^2$  carbon. However, only  $\pi$ -bond electrons and lone pair electrons can move since they still have an extra set of electrons that can be shared. Due to delocalization, molecules resonance stability and the wavelength range of light absorption of molecules in the spectrum can be determined.

Bakhshi and Bhalla (2004) had stated that electrical conductivity of organic conjugated polymer can increase dramatically on treatment with oxidizing and reducing agents. Oxidation and reduction reactions are termed as *p*-doping (electron-accepting) and *n*-doping (electron-donating) respectively. A charge transfer reaction involves in the doping reaction and the process is more accurately classified as redox process as shown in general scheme below.

For *p*-doping process:



For *n*-doping process:



where *X* is oxidizing agents, *M* is reducing agents and *n*<sup>+</sup>/*n*<sup>-</sup> is ionic charge of molecule. Bakhshi and Bhalla (2004) also mentioned that the reactions above commonly occur in unsaturated polymers since their  $\pi$ -electrons can be easily added or removed to the polymeric chains thus increasing electrical conductivity. Besides that, these polymers can either be electron donors or electron acceptor depending on their individual characteristics. Since HOMO is mainly located at donor unit and LUMO is mainly located at acceptor unit (Zhang and Wang, 2012), donor polymers is necessary to have high HOMO energy. In fact most of them are planar and posses symmetric geometries that benefit for intramolecular and intermolecular ordering of the polymer chains in solid state. However, acceptor polymers have lower LUMO energy level and posses at least one or more strong electron-withdrawing groups. They are coplanar and symmetric, which is important for the properties of copolymer (Guo *et al.*, 2013).

Conjugated polymers can be modified to reach desired applications. It is strictly important to keep in mind that there are five factors dependant on each other and must be inclusively considered for specific applications: (1) types of side chain, (2) high molecular weight, (3) band gap and absorption behavior, (4) HOMO and LUMO energy levels, and (5) suited morphology with low barriers. Besides improving the solubility and increases the molecular weight of conjugated polymers, side chain also plays a significant role in influencing intermolecular interactions thus leading changes in morphology and charge carrier mobility. The emitting color of organic light-emitting diodes (OLED) and the open-circuit voltage ( $V_{oc}$ ) in OSC can be tailored through desired light absorption by tuning the energy band gap. This change will influence HOMO and LUMO levels. To pursuit an ideal conjugated polymer for specific applications, it is therefore necessary to balance these designing principles (Guo *et al.*, 2013).

### 2.3.1 Polypyrrole

Pyrrole is a heterocyclic aromatic organic compound with formula  $C_4H_4NH$  (Loudon, 2002). Due to delocalization of the lone pair of electrons of the nitrogen atom in the aromatic ring, pyrrole has very low basicity and very weak base with  $pK_{aH}$  of about -1 and -2. Pure colorless pyrrole turns brown over time due to accumulation of impurities. However, it can be purified by distillation immediately before use.

Polypyrrole (PPY) is formed from polymerization of pyrrole with nitrogen located in an aromatic cycle. PPY is an insulator but attractive as an electrically conducting polymer because of its relative ease of synthesis. Conditions and reagents used in oxidation

affects the conductivity of material. PPY films are yellowish but due to some oxidation they turn darken as exposed in air. The degree of polymerization and film thickness attribute to blue and black color of doped films.

As mentioned by Hosseinl (2007), pyrrole reacts very rapid with aqueous ferric chloride and produced black powder which is insoluble in all common solvents. Due to its insolubility and infusibility, this conducting polymer is poorly processable either by solution technique or by melt processing method (Wusheng *et al.*, 2001). However the improvement of mechanical and optical properties, together with stability and processability of this material can be achieved by forming copolymer of pyrrole, or by forming PPY composites or blending with soluble matrix polymers or inorganic materials (Hossein, 2007). Figure 2.6 below shows the monomer repeated unit of PPY.

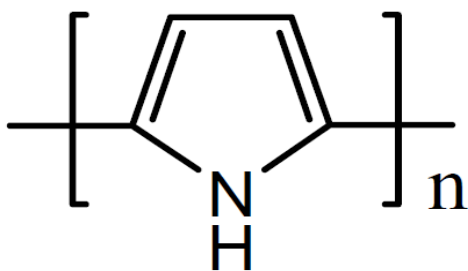


Figure 2.6: Monomer repeat unit of Polypyrrole (Chen, 2007).

### 2.3.2 Polythiophene

Polymerization of thiophenes with formula  $C_4H_4S$  forms PT that contains sulfur in an aromatic cycle.

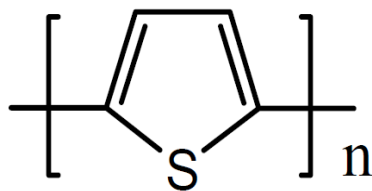


Figure 2.7: The monomer repeat unit of PT (Chen, 2007).

At room temperature, thiophene is a clear color liquid with mildly pleasant odor. Through theoretical calculations, Treiber *et al.* (1997) suggest that the degree of aromaticity thiophenes is less as the consequence of the „electron pairs“ on sulfur are significantly delocalized in the  $\pi$ -electron system. In fact it is difficult to dilute this material by simple distillation due to the high reactivity of thiophene toward sulfonation. Thiophene rings can be coplanar due to the overlap of  $\pi$ -orbitals of the aromatic rings. The increasing number of coplanar rings attributes to the longer conjugation length and materials absorb longer wavelength thus lowering the separation between adjacent energy levels. The mislinkages during synthesis and bulky side chains are some factors resulting in permanent coplanarity. However the environmental factors such as solvent, temperature, application of an electric field and dissolved ions can twist the conjugated backbone. This will reduce conjugation length and cause an absorption band to shift. Polythiophene has low conductivity in its unsubstituted condition but become conductive and high environmental stable after doping.

A research done by Borrelli *et al.* (2012) had fabricated multilayer PT based organic solar cell when PT thin film was deposited on ITO-coated glass substrate for incorporation as electron donor layer. The device structure was ITO/PT/C<sub>60</sub>/BCP (8 nm)/Ag (100 nm) where fullerene (C<sub>60</sub>) act as the electron acceptor, bathocuproine

(BCP) as an exciton blocking layer, and silver (Ag) as the cathode. By varying thickness of PT and C<sub>60</sub>, the best device performance with PCE 0.8% was achieved using about 25 nm of PT and 30 nm of C<sub>60</sub>.

Haeldermans *et al.* (2008) had shown that the use of (poly[3-(sodium-6-hexanoate)thiophene-2,5-diyl]) (P3SHT) as photosensitizer in liquid electrolyte based PT-sensitized solar cells had increased PCE to 0.37% compared to (poly(3-hexyl thiophene)) (P3HT)-sensitized solar cell with PCE of 0.05%. By spin-coating both films on titanium dioxide (TiO<sub>2</sub>), the interactions between polymer P3SHT and TiO<sub>2</sub> endured a conformation change into a more twisted polymer backbone thus leading to a reduction to the main conjugation length and observing a blue-shifted in absorption spectrum (Luzzati *et al.* (2002) and Kim *et al.* (2003)). Besides Coakley *et al.* (2003), Goh *et al.* (2007) and Liu *et al.* (2006) had stated that the presence of the carboxylate group enhanced the interface between the PT and TiO<sub>2</sub>, causing a better polymer infiltration in the porous titania layer and a better charge transfer. Figure 2.8 below shows chemical structure of P3SHT.

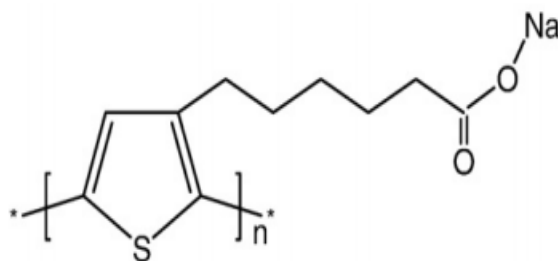


Figure 2.8: Chemical structure of P3SHT. Due to the extra carboxylate group on the side chain this polythiophene dissolves in water (Haeldermans *et al.*, 2008).

### 2.3.3 Poly (3-thiophene acetic acid)

Poly (3-thiophene acetic acid) (P3TAA) is one of PT derivatives with the substitution of acetic acid side chain that is covalently bound to polymer as shown in Figure 2.9.

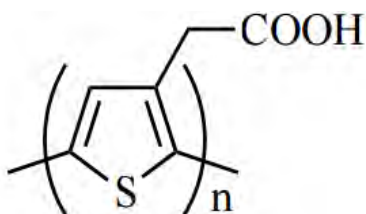


Figure 2.9: Monomer repeat unit of P3TAA (Yanagida *et al.*, 2004).

Acetic acid is the simplest and smaller of carboxylic acid, and smaller carboxylic acids (contain 1 to 5 carbons) are soluble in water. The presence of hydrogen bonding in acetic acid increases the crystallinity degree of this polymer thus increasing its solubility. Miller-Chou & Koenig (2003) has stated that it is possible to dissolve a crystalline polymer at room temperature because of the ability of solvent materials to interact with its chain through hydrogen bonding. Rather than long branched polymer, short branched polymer such as P3TAA is one of the factors causing it to be soluble in most common solvents. P3TAA solution dilutes in acetonitrile has yellowish color.

The solubility of pure P3TAA and protonated P3TAA in 37% hydrochloric (HCl) aqueous solution were investigated by Giglioti *et al.* (2004) in various solvents. It was reported that the solubility of P3TAA in common solvents increased after being treated in HCl solution. Both pure and protonated P3TAA were soluble in ammonium hydroxide (NH<sub>4</sub>OH) only with pH  $\geq$  11 and the highest solubility was observed in



N-dimethylformamide (DMF) solvent. However, pure P3TAA was not soluble in chloroform (CHCl<sub>3</sub>) even after being protonated in HCl.

In 2004, P3TAA and its co-polymer, poly(3-thiophene acetic acid)–poly(hexyl thiophene) (P3TAA-PHT) were deposited on nanoporous titanium dioxide (TiO<sub>2</sub>) electrode as an active layer for organic solar cells separately by Yanagida and his group. It was reported that device with P3TAA had higher PCE value compared to P3TAA-PHT device. In fact, the cell performances dramatically enhanced with the addition of ionic liquid 1-methyl-3-n-hexylimidazolium iodide into the electrolyte (MHlml). The PCE of both cells had increased from 1.1% to 2.4% and 0.9% to 1.6% respectively. Other device parameters can be observed in the Table 2.1.

Table 2.1: Organic solar cells parameters of the cells fabricated with polymer dyes (Yanagida *et al.*, 2004).

	P3TAA dye		P3TAA-PHT dye	
	With MHlml	Without MHlml	With MHlml	Without MHlml
<b><math>J_{SC}</math> (mA/cm<sup>2</sup>)</b>	4.14	9.74	5.06	7.00
<b><math>V_{OC}</math> (mV)</b>	420	405	382	375
<b>FF</b>	0.63	0.60	0.45	0.62
<b>PCE (%)</b>	1.10	2.40	0.90	1.60

Recently, many studies were successfully examining the organic dyes with carboxylic groups as an effective sensitizers to the mesoporous TiO<sub>2</sub> (Hara *et al.*, 2000, Hara *et al.*, 2001a and 2001b).

## 2.4 Chlorophyll

Chlorophyll is an efficient organic semiconductor in light absorption and has green pigments that play a central role in natural photosynthetic system. There are two major groups in CHLO; CHLO a and CHLO b.

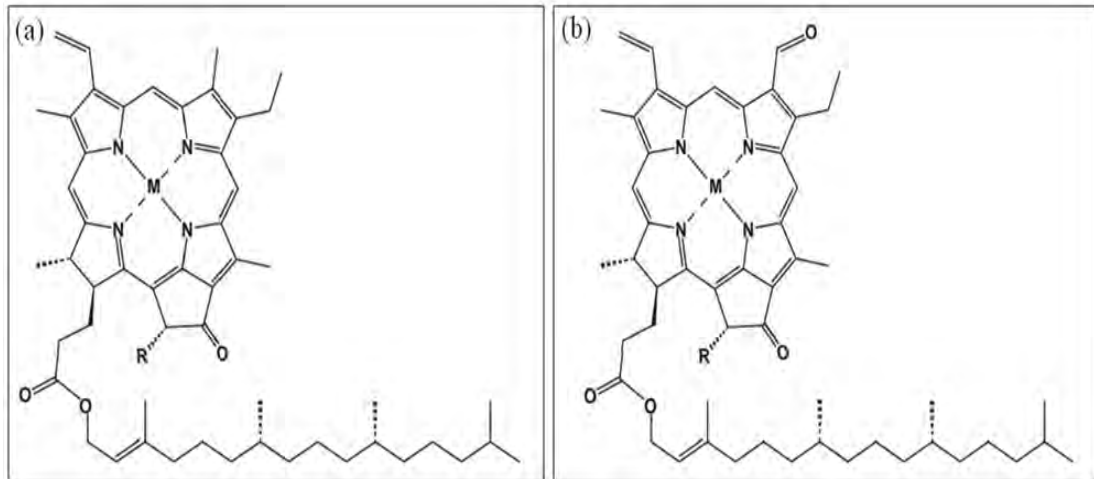


Figure 2.10: Structure of CHLO a (a) and CHLO b (b) (Kashiyama *et al.*, 2013).

As shown in Figure 2.10 above, they only differ slightly in the composition of side chain. CHLO a absorbs light within violet, blue and red wavelengths and the presence of CHLO b next to CHLO a extends the absorption spectrum while mainly reflecting green spectrum. This reflectance is the reason CHLO appears in green color to viewer's eyes. The absorbance spectra of both types of CHLO are shown in Figure 2.11. The maximum spectra absorbance of CHLO a are at wavelength 436 nm and 666 nm whilst CHLO b are at wavelength 452 nm and 642 nm. The total wavelength for both CHLO has widened the range of spectra absorbance and suitable to be used as photon receptor in organic solar cells architecture.

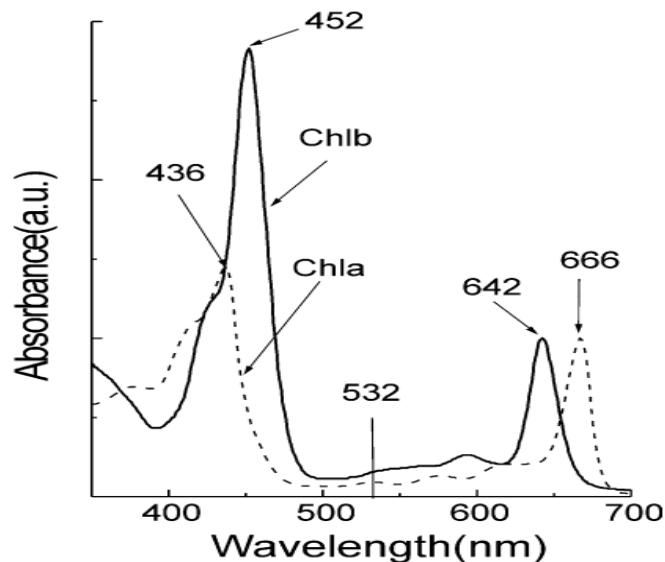


Figure 2.11: Absorbance spectra of CHLO a and CHLO b (Sun & Wang, 2004).

A network of alternating single and double bonds inside CHLO together with delocalize orbital for stabilizing the structure is a consequence to a very effective photoreceptor (Hasiah and Senin, 2007). Besides, Tamiaki *et al.* (2007) has stated that the photochemical and photophysical properties of CHLOs can be tailored as desired by using molecular engineering. The capability of CHLOs in harvesting light, transferring energy as well as electrons, due to their intrinsic p/n ambipolar properties, has offered a significant promise in various applications, such as photodynamic therapy and photovoltaics (Li *et al.*, 2007, Wang and Tamiaki, 2010 and Wang *et al.*, 2013b).

In 2013a, Wang and his group had used CHLO derivative, chlorin  $e_6$  as photo-sensitizer in dye-sensitized solar cells (DSSC). Due to its carboxylate binding units, the chlorin has a strong tendency to form aggregate on semiconductor surfaces. In order to overcome this barrier, Wang *et al.* (2003a) had engineered chlorin  $e_6$  molecular by introducing alkyl ester substituents at the C15 position of the chlorin macrocycle which

later on change to C17 position. This relocation had increased the short circuit photocurrent ( $J_{SC}$ ),  $V_{oc}$  and the PCE of DSSC from 2.5 mA/cm<sup>2</sup>, 0.47 V, and 0.9% to 6.6 mA/cm<sup>2</sup>, 0.60 V, and 2.9%, respectively. The carboxy group was then relocated and the cyclic  $\pi$  system was extended on C3-substituent. The PCE was further increased to 6.7% with  $J_{SC} = 15.6$  mA/cm<sup>2</sup>,  $V_{oc} = 0.65$  V, and FF = 0.66. This improvement was due to charge recombination reduction between the TiO<sub>2</sub> semiconductor and redox couple in the electrolyte as well as the enhanced electron-injection and light-harvesting efficiencies.

Studies from Khairul *et al.* (2013) and Rafizah *et al.* (2013) stated that the presence of spin-coated CHLO thin film on thiourea based organic solar cells had increased the conductivity of thin films under various light intensities. The highest values were observed at maximum intensity (100 Wm<sup>-2</sup>) with 0.1472 Scm<sup>-1</sup> and 0.1377 Scm<sup>-1</sup>. From these studies, it shows the capability of CHLO to harvest light into solar cells and majorly distributed by the wide range in spectrum absorption.

## **CHAPTER 3**

### **METHODOLOGY**

This chapter explains the procedure that have been done and equipments that have been used during the experiment and the study. The flowchart and figures of procedure are also provided so the process can be more easily understood.

#### **3.1 Sample Preparation**

##### **3.1.1 Cleaning ITO slides**

All ITO slides and Quartz slides were cleaned by using JEIOTECH US-05 Ultrasonic Cleaner (5L) at room temperature. The ultrasonic waves, usually at frequency between 20 kHz and 50 kHz was generated by an electric ultrasound generator were led to the production of compression and vacuum waves at a very high speed by a transducer mounted under the bottom of a stainless steel tank. During the vacuum phase, cavitation occurred where a numerous microscopic bubbles of gas were formed in the liquid. As the waves continuing produced, an enormous pressure were exerted on cavitation bubbles making them oscillate faster and grow to an unstable size thus increasing the temperature of gas containing in it untill the bubbles collapsed on itself with enormous

energy. The implosion had caused the impact energy hit the surface of ITO slides and Quartz slides to be cleaned, interacting both physically and chemically. Slides were placed in the beaker filled with solvent and the beaker was then inserted in the removal basket inside the tank that was filled with tap water. The level of solvent in the beaker was totally immersed under the level of tap water. Slides were placed with ITO layer facing up the bottom of beaker during the process for an optimal cleansing.

The cleaning process started with distilled water, followed by DECON 90 detergent and then distilled water, continued with acetone and finished with distilled water. Each solvent was set for 10 minutes cleansing process respectively. DECON 90 detergent was used as a solvent to break down the surface tension of water base and to cavitate efficiently. The temperature of tap water in the tank was continually observed to avoid it reaching 56°C, the boiling point of acetone where at that state the intensity of cavitation stops. The excess water on slides was instantly dried out by using regular hair dryer to avoid contamination.

### **3.1.2 Etching ITO layer on glass substrate**

ITO layer removal was done by using aqua regia solution in the the fume hood with extreme caution. This yellow-red solution which also known as nitro-hydrochloric acid is a highly corrosive fuming mixture of acids. Aqua regia solution was prepared by mixing 6 ml of concentrated hydrochloric acid and 2 ml of concentrated nitric acid, optimally at volume ratio of 3:1. Nitric acid was added to hydrochloric acid very slowly to avoid any sudden explosion. The combination of these two strong acids could rise the

temperature up to more than 100°C. The solution was leaved in an open container to cool it down. A small amount of solution was then poured into a beaker untill 5% of ITO slide immersed in the solution. For a perfect clear ITO removal, half the effectiveness of aqua regia solution was reduced by keeping it in a tightly closed glass bottle in the fume hood at room temperature for about 2 to 3 days. The ITO slide was placed leaning onto the inside beaker with ITO layer facing up the solution so the formation of toxic gases will not dissolve other part of the layer. Figure 3.1 shows the illustration of ITO layer etching process. The slide was left in the solution for about 20 minutes and then cleaned with distilled water and acetone. Hair dryer was used to dry out the slide. The aqua regia solution cannot be stored for a long time and only a needed amount was prepared and the excess solution was neutralized with sodium bicarbonate and disposed in the drain followed by a large amount of water.

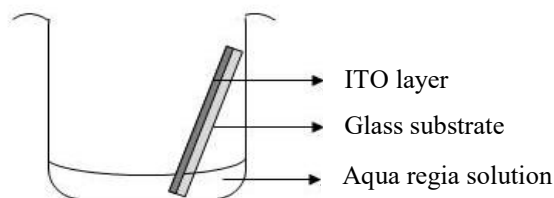


Figure 3.1: Illustration of ITO layer etching process.

### 3.1.3 Single layer thin film deposition

Single layer thin film of P3TAA, PPY, PT and CHLO was deposited on ITO glass substrate by electrochemistry method using Electrochemical Impedance Spectroscopy (EIS) PGSTAT 302 at room temperature. A typical electrochemical impedance experimental set-up consists of an electrochemical cell (the system under investigation),

a potentiostat/galvanostat and a General Purpose Electrochemical System (GPES). Three-electrode configuration was used in this electrochemical cell set-up consists of working electrode (WE), counter electrode (CE) and reference electrode (RE). In potentiostatic mode, the potential of CE against WE was accurately controlled by a potentiostat/galvanostat (PGSTAT) correspond to the applied potential whilst the potential difference between WE and RE was well defined. In galvanostatic mode, the current flowed between WE and CE was controlled.

In three-electrode configuration, the platinum CE was used to close the electrical circuit in the electrochemical cell by carrying current to WE. ITO slide acted as WE in this set-up, the electrode under investigation where a single layer thin film deposition occurred on ITO layer. Since the absolute potential of a single electrode cannot be measured, the silver chloride electrode (Ag-AgCl) RE with a stable and constant electrode potential was used. All these electrodes were immersed in the solvent during depositon procedure as illustrated in Figure 3.2. Types of solvent depend on type of thin film that was going to deposit.

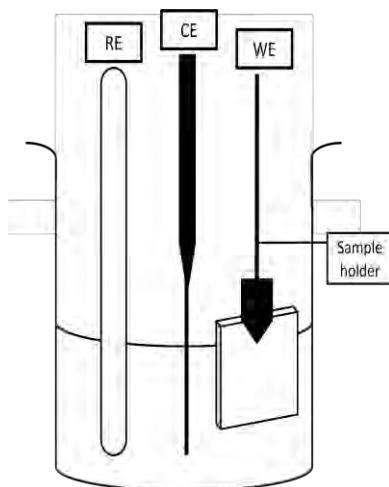


Figure 3.2: Illustration of electrochemical cell under three electrode configuration.



By using the GPES method software, cyclic voltammetry (staircase) method was set to be as shown in Table 3.1. The cyclic of the process was set at the „Measurement“ column for 5 scans. The difference of film thickness were determined by the number of cyclic. In order to avoid the same current and voltage as the one in ITO layer, thin film was not deposited less than 5 scans where the edge probes during characterization could penetrate further into ITO layer.

Table 3.1: Procedure set for cyclic voltammetry (staircase) method.

<b>Parameter setup</b>	<b>Value of parameter</b>
Start potential (V)	-2.00
First vertex potential (V)	-2.00
Second vertex potential (V)	1.50
Step potential (V)	0.01
Scan rate (Vs <sup>-1</sup> )	0.05

### 3.1.4 Coating chlorophyll thin film

Conjugated polymer layer was coated with CHLO thin film by using Laurell Spin Coater of model WS-400BZ-6NPP-Lite. Before starting the coating process, the inner part of the bowl and the surface on spin chuck were cleaned to avoid contaminations. Substrate was placed on spin chuck and the vacuum button was turned so substrate got stuck tightly on the chuck during coating process. A small puddle of polymer/CHLO solvent was dispersed near the center of substrate surface. Three rates of speed were used to complete one cycle. Each thin film was coated on substrate by repeating three cycles of rotation.

The first rate was set to 500 rpm for 10 seconds in order to spread the solvent over the entire substrate thus resulting in less waste of resin material. The second rate was set to 1000 rpm for 25 seconds where thin film was coated at this rate. In general, the higher the spin speeds, the longer the spin times create thinner films. Last rate was then set to 2000 rpm for 30 seconds. At this rate, the exceed solvent was drying out as it was spreading off the edge of substrate. The selection of spin rate was referred to the range used in Ogi *et al.* (2007) and Shinde *et al.* (2015) studies. The cycle was then repeated three times for each solvent. The bowl lid was remaining closed during coating process to minimize the unwanted turbulence. By spinning in a closed bowl the vapors of the solvents in the resin itself were retained in the bowl environment and tend to cover the affects of minor humidity variations. This variations and turbulence caused by the presence of operators and any other equipment were eliminated from the spin process. After all thin films were coated; all substrates were heated in a furnace at temperature 50°C for 10 minutes to improve the crystallization of thin films for a better charge transport. An Al electrode was then deposited on top of these CHLO thin films by using physical vapor deposition (PVD). Figure 3.3 shows the illustration of a complete fabricated organic solar cell.

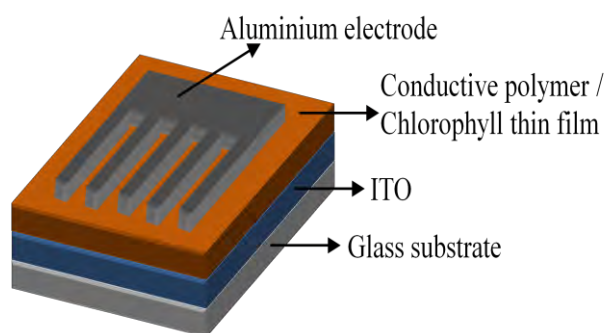


Figure 3.3: Illustration of organic solar cell.

## **3.2 Sample Characterization**

### **3.2.1 Thickness measurement**

The thickness of single layer thin film deposited on ITO coated glass substrate was measured by using VEECO Dektak 150 Stylus Surface Profilometer together with Detak 150 software at Physical Sciences Department in University Kebangsaan Malaysia (UKM). Firstly the substrate was placed on the center of sample stage and turned on the stage vacuum. The stage was then rotated to the desired orientation so that the features to be measured were facing perpendicular to the scan direction. The scan location and length was defined by using software in the computer, started from surface with no thin film towards the area deposited with thin film. As the scan button was clicked on, the stylus physically making contact with the substrate surface and moving the stage front to back as stylus was held statically in place to measure changes in surface height. The door of equipment was remaining closed during scan process. The thickness measurement was analyzed by using two cursors visible on the computer screen: reference cursor (R-cursor) and measurement cursor (M-cursor). The R-cursor was placed at the bottom of the step in the image and the M-cursor was placed at the top of the step (see Appendix F). Through Dektak 150 software the value was the automatically displayed on the computer sreen. Five readings were taken at five different areas on each surface of thin film. The average and the standard deviation were then calculated.

### 3.2.2 Energy band gap measurement

Energy band gap of conducting polymers thin films, CHLO thin film and combination of both were measured by using Perkin Elmer's instrument model Lambda 25 UV-Vis (Ultraviolet-Visible) spectrometer. Thin films were deposited on Quartz slides for an optimum measurement. The operation was done in ultraviolet (UV) range at room temperature, starting from 190 nm to 1100 nm of wavelength. Halogen lamp and deuterium lamp were used as sources to produce the desired radiation in UV range. Two blank samples (blank Quartz slides) were firstly inserted in sample compartment as a reference to other sample's measurement. There are two stages inside sample compartment where the front stage is for the characterized sample and the one at the back is for the reference sample (see Appendix G).

The radiation produced was dispersed at monochromator to produce spectrum, and then splitted into two directions at beam splitter. One of them was passing through characterized sample and the other was passing through reference sample. Both radiations were finally directed into photodiode detectors. When the scanning sample finished, a graph of thin film absorbance,  $A$  versus wavelength,  $\lambda$  was then displayed on computer screen through Lambda 25 software. Energy band gap was then calculated by using Equation 3.1.

$$E_g = \frac{hc}{e\lambda} \quad (3.1)$$

The symbol  $h$  is Planck's constant ( $6.63 \times 10^{-34} \text{ kgm}^2\text{s}^{-1}$ ),  $c$  is speed of light ( $3 \times 10^8 \text{ ms}^{-1}$ ) and  $\lambda$  is wavelength in nanometer. Equation 3.1 is divided with charge of electron,  $e$  ( $1.602 \times 10^{-19} \text{ C}$ ) to convert the unit of energy band gap,  $E_g$  to eV.

The graph of  $A^2$  versus  $E_g$  was then plotted and the  $E_g$  for each thin film was obtained by linearly extrapolating the absorption curves in the abrupt absorption region to the horizontal ordinate axis.

### 3.2.3 Electrical conductivity measurement

Jandel Universal Probe Station together with RM3000 test unit equipment were used to determine electrical conductivity of thin films. In order to start the procedure, ITO substrate was placed on sample stage with thin film layer facing upward. Four probes were then released slowly until they touch the surface of thin films without penetrating into ITO layer. The red knob was pushed with slight pressure to release these probes. Current of 1 mA was applied through RM3000 test unit and various value of voltage were displayed on its screen. Ten values of voltage were collected at five different points on each ITO substrate. The lid of probe station was closed during operation under dark condition. Under different illumination, the intensity of four regular light bulbs was controlled in order to produce 20 W/m<sup>2</sup>, 40 W/m<sup>2</sup>, 60 W/m<sup>2</sup>, 80 W/m<sup>2</sup> and 100 W/m<sup>2</sup> of intensity. Five variations of light intensities were used to investigate their effect on electrical conductivity of thin films. Since the characterization of cells was for laboratory scale, the maximum intensity was set at 100 Wm<sup>-2</sup>.

Five different areas were randomly selected on each thin film surface. At each area, current of 1 mA was applied and a series of voltages were displayed on Jandel RM3-ar test unit. Ten values were then collected and the average was calculated.

The sheet resistivity,  $R_{st}$  was calculated by using Equation 3.2.

$$R_{st} = \left(\frac{V}{I}\right) 4.532 \quad (3.2)$$

where  $I$  refers to a fixed current in mA and  $V$  is voltage gathered from Jandel RM3-ar test unit. Since the thickness of film deposited is in nanometer, much smaller compared to the space between two probes of conductivity measurement instrument, the film is considered as an infinite sheet. The correction factor used for infinite sheet is 4.532 as in Equation 4.2 above. The graph of electrical conductivity,  $\sigma$  versus light intensity for each thin film was plotted by calculating the  $\sigma$  using Equation 3.3.

$$\sigma = \frac{1}{R_{st}} \quad (3.3)$$

#### **3.2.4 Power conversion efficiency measurement**

Current-voltage (I-V) characteristic of single layer and double layer thin films organic solar cells were determined by using Keithley two point probes method of model 4200 SCS's (Semiconductor Characterization System) Source Measure Units (SMUs). The sytem was connected to a computer and a probe station. Before starting the procedure, the system was turned on for 15 minutes to stabilize it. A four-wire method, connected

to two needles (probes) was made to eliminate the lead resistance that could otherwise affect the measurement accuracy. The schematic diagram is shown in Figure 3.4.

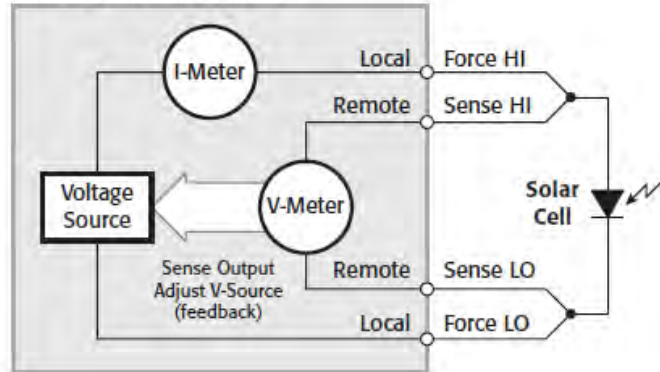


Figure 3.4: Schematic diagram of of 4200-SCS's SMU to solar cell connection.

The cell was then placed on probe station with probe 1 touched ITO layer and probe 2 touched Alluminium electrode. A voltage was sourced across the cell using Force HI and Force LO, and the voltage drop across the cell was measured through Sense HI and Sense LO. Those two probes were adjusted using the turning knob until they slightly touched the layer surface, not penetrating into the layer. The SMU was setup to source a voltage sweep starting from -5 V until +5 V and then measure the resulting current. Probe station was covered with thick dark plastic for procedure under dark condition. The intensity of regular light bulb was controlled for procedure under different illumination, starting from  $10 \text{ W/m}^2$ ,  $30 \text{ W/m}^2$ ,  $60 \text{ W/m}^2$  and  $100 \text{ W/m}^2$ . The 4200-SCS system was running with KITE Software and the I-V curve of PV forward biased together with data sheet were displayed on computer screen once the scan onto cell completed. The device parameters  $I_{SC}$ ,  $V_{OC}$ ,  $I_m$ ,  $V_m$ ,  $P_m$ , FF and efficiency were then determined and calculated using equations shown in previous chapter.

### 3.2.5 Hall Effect measurement (HEM)

All samples that were going to be characterized were first prepared according to the standard procedure of HEM. For an accurate result, samples were made sure to have well-defined geometries called van der Pauw (vdP) geometry and good ohmic contacts. In order to do so, samples must be connected to the sample holder. The back side of ITO substrates were firstly attached to the samples holder by using a regular selfon tape. A small amount of solder material; in this study we used solder paste was placed on every edge of substrate containing sample to be characterized. Four thin wires with a proper length were used to connect the substrate to the sample holder. One end of each wire was placed at all four proper substrate contact points respectively by using tweezers. The other end of wire was then connected to the contact point on sample holder by using solder paste. Figure 3.5 shows the illustration of substrate mounted on the sample holder. The connection was then tested by using multimeter.

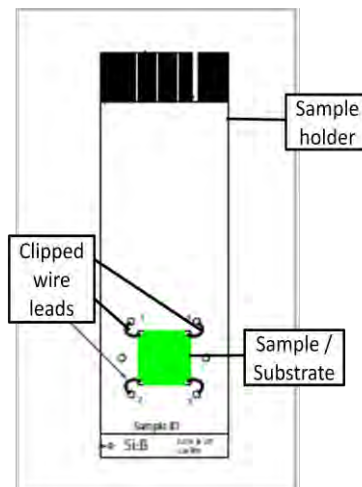


Figure 3.5: Sample holder with mounted substrate and leads.



The characterization was done by using Hall Effect Measurement System model 7600 supplied by Lakeshore Ltd. The measurements consist of two parts and were performed using the Leois-JSF software. All experimental steps including data acquisition were controlled by a computer. The sample was then inserted in the sample enclosure. It is important to remain the chiller temperature always below the room temperature to avoid any damages to the instrument. The I-V curve traces measurement was first done to define the ohmic contact of sample. Only samples with good ohmic contact could be proceeded to the next step.

When a magnetic field of 1 Tesla is applied, the production of a voltage difference (Hall voltage)  $V_H$  across a device was calculated using Equation 3.4 and 3.5 by substituting data collected (as shown in Appendix A).

Total Hall voltage,  $V_{H\ total}$  :

$$V_{H\ total} = V_{+31,42(+B)} - V_{+31,42(-B)} + V_{-31,42(+B)} - V_{-31,42(-B)} + V_{+42,13(+B)} - V_{+42,13(-B)} + V_{-42,13(-B)} - V_{-42,13(+B)} \quad (3.4)$$

And therefore, the average of Hall voltage,  $V_{H\ avg}$ :

$$V_{H\ avg} = \left( \frac{V_{H\ total}}{8} \right) \quad (3.5)$$

The calculation for Hall coefficient in vertical ( $R_{HC}$ ) and horizontal ( $R_{HD}$ ) directions are given as Equation 3.6 and Equation 3.7 respectively.

$$R_{HC} = \left\{ \frac{V_{+31,42(+B)} - V_{-31,42(+B)} + V_{-31,42(-B)} - V_{+31,42(-B)}}{I} \right\} \quad (3.6)$$

and;

$$R_{HD} = \left\{ \frac{V_{+42,13(+B)} - V_{-42,13(+B)} + V_{-42,13(-B)} - V_{+42,13(-B)}}{I} \right\} \quad (3.7)$$

Here,  $I$  is the value of current applied. The details of input parameters for I-V curve traces are listed in Table 3.2 and Table 3.3 with no magnetic field, 0 kG and at variable magnetic field, 1 kG – 10 kG respectively. The current was fixed at 0.1 A for both input parameters.

Table 3.2: Input parameters for IV curve traces.

Items	Input parameters	Set value
<b>IV curve traces</b>	Start current (A)	0.001
	Stop current (A)	0.050
	Step current (A)	0.005
	Voltage compliant (V)	20
	Number of points	10
	Delay time (s)	0.002

Table 3.3: Input parameters for variable magnetic field measurement.

Items	Input parameters	Set value
<b>Vriable magnetic field</b>	Start magnetic field (kG)	1
	Stop magnetic field (kG)	10
	Step magnetic field (kG)	1
	Voltage compliant (V)	10
	Number of points	0.100
	Current, I (A)	20
	Delay time (s)	0.002

Figure 3.6 shows the flowchart of the overall methodology.

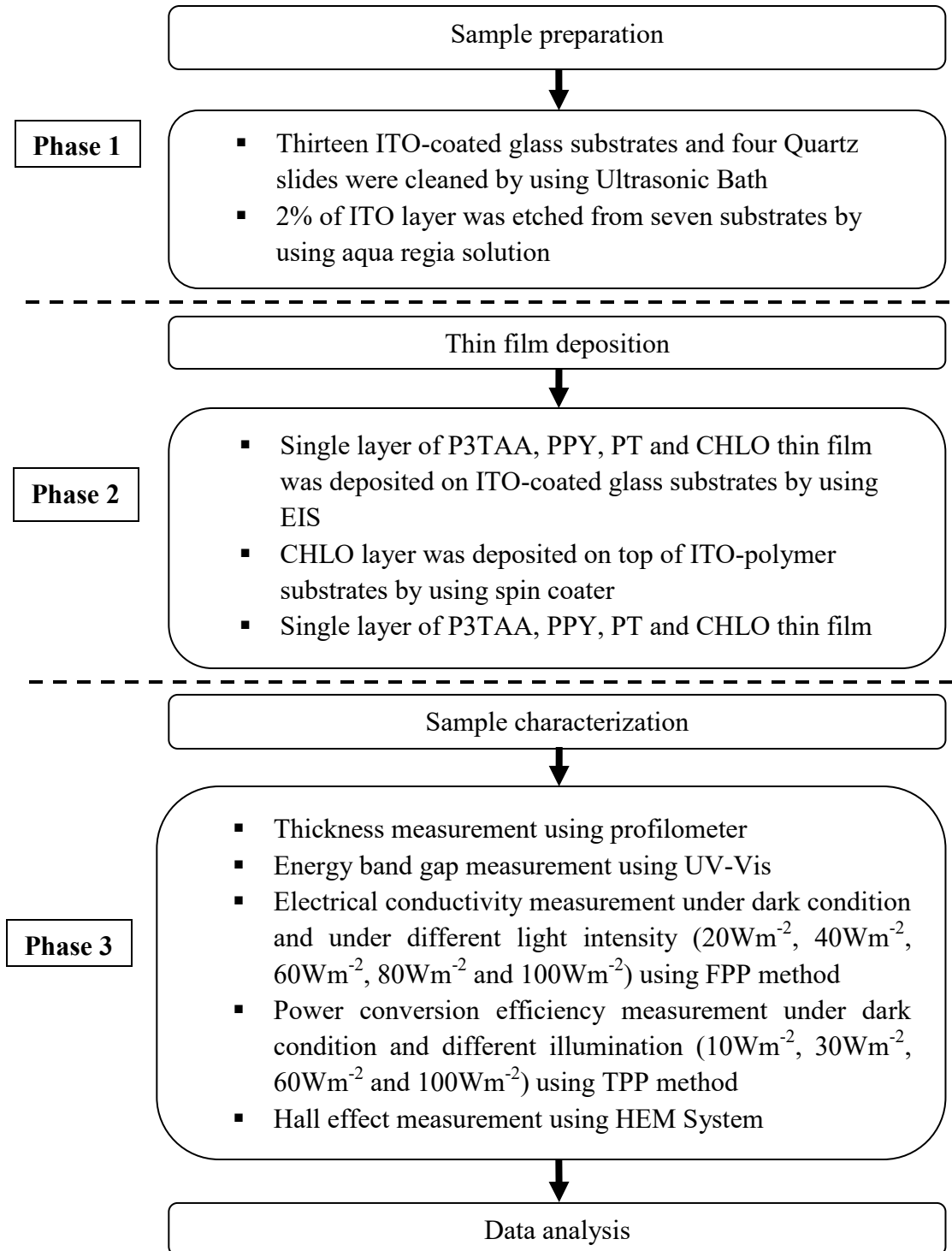


Figure 3.6: Flowchart of methodology.

## CHAPTER 4

### RESULTS AND DISCUSSION

This chapter will discuss all results that have been carried out from this study. Results of thickness measurement, energy band gap, electrical conductivity, Hall Effect measurement and power conversion efficiency together with related tables and figures are all included for a better understanding on the outcome of this study.

#### 4.1 Thickness Measurement

Single layer thin films thickness is determined using profilometer. Generally Faraday's law considers that deposited metal film are both compact and homogeneous but not for polymer films where their thickness are inconsistent. Viau *et al.* (2014) has reported that it is more suitable to use profilometer to measure polymer films thickness.

Table 4.1: Thickness of polymers thin film and chlorophyll thin film deposited on ITO coated glass substrate.

Sample	Thickness (nm)
CHLO	72.6 ( $\pm$ 20.5)
P3TAA	97.1 ( $\pm$ 37.2)
PPY	50.5 ( $\pm$ 14.7)
PT	64.4 ( $\pm$ 30.9)

The average and their standard deviation for each sample are shown on Table 4.1. The average thickness of thin film is different comparing to one another. Majority thickness of CHLO thin film, PPY thin film and PT thin film are in range of 50 nm to 70 nm. A maximum absorption of photons is required for an optimum performance of organic solar cell. Typically, the absorption coefficient of organic materials are  $10^5 \text{ cm}^{-1}$  thus the optimal thickness of 100 nm organic layer is necessary to allow maximum absorption in visible region when a reflective back contact is used as reported by Gupta *et al.* and Apaydın *et al.* on 2013. With an average of 97.1 nm, P3TAA thin film has the finest thickness compared to others. Whilst PPY thin film is the thinnest one with thickness average of 50.5 nm which will limit the possible absorption of incident light.

Average thickness for CHLO thin film and PT thin film are 72.6 nm and 64.4 nm respectively. The reading for each area taken on one surface of thin film is dissimilar and some even with huge gap between the readings. This shows that the thin film does not distribute uniformly on the ITO slide. It might be a consequence of formation small nodules at early stage of electropolymerization conjugated polymer films on substrate. From the aggregation of these small nodules, polymer continues to grow forming islands (Chainet & Billon, 1998). The increasing of island boundaries among each other

might be a reason for a huge gap between thickness measurements on each film surface. Furthermore even the same method, same parameter set and same solvent are use to deposit these thin films, types of materials alone is able to differentiate thickness and morphology of films during fabrication.

Tsuchiya *et al.* (2002) has stated 1  $\mu\text{m}$  films as thick films. Therefore all films fabricated in this study can be classified as thin films since all average thicknesses measured are thinner than 1  $\mu\text{m}$ .

## **4.2 Energy Band Gap Measurement**

The spin coated CHLO thin film deposition on top of polymers thin film brings difference to the value of energy band gap. Energy band gap of P3TAA thin film before and after depositing CHLO layer can be seen in Figure 4.1.

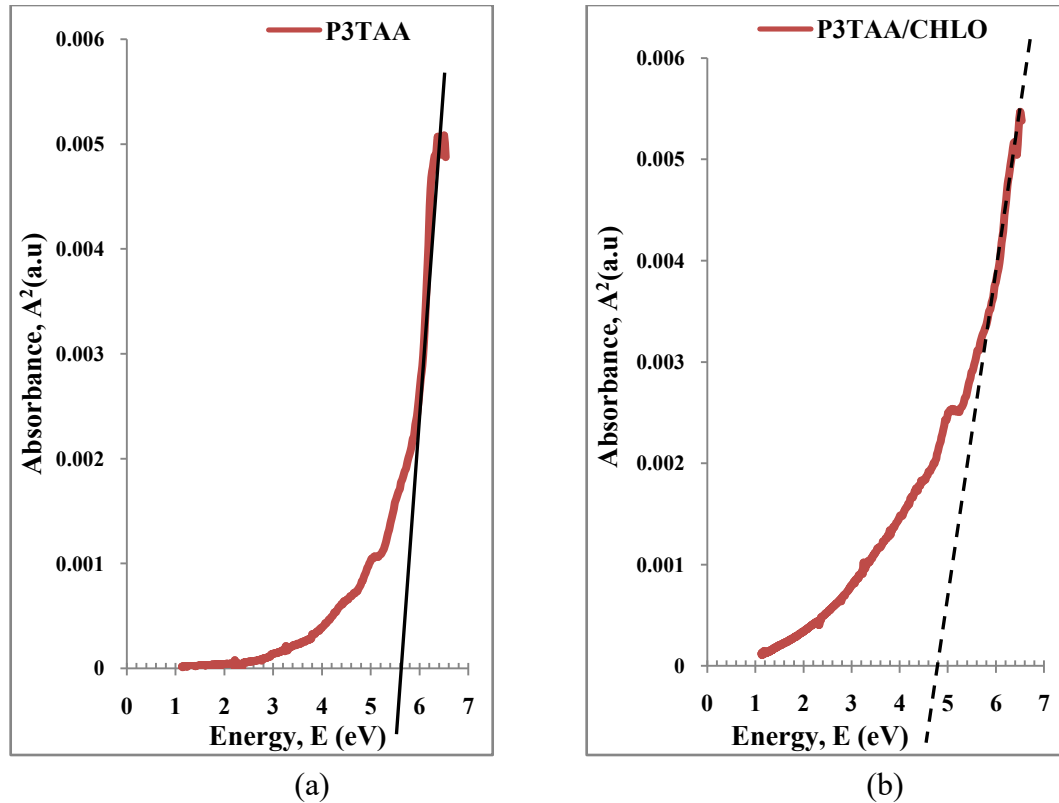


Figure 4.1: Energy band gap of P3TAA single layer thin film (a) and energy band gap of P3TAA/CHLO layer by layer thin film (b) on Quartz slides.

As shown in Figure 4.1, energy band gap ( $E_g$ ) of P3TAA single layer thin film is 5.6 eV. However after depositing CHLO layer on top of it, the  $E_g$  reduces to 4.8 eV. This shows a huge difference with total of 0.8 eV between those two measurements.

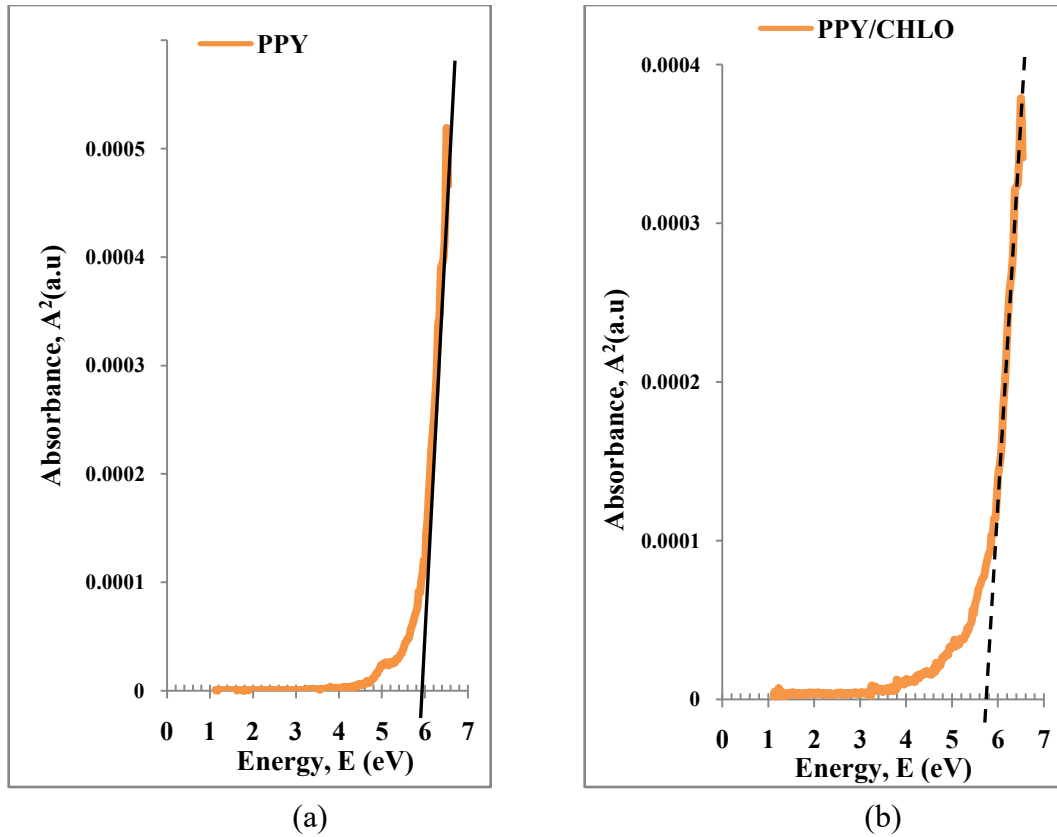


Figure 4.2: Energy band gap of PPY single layer thin film (a) and energy band gap of PPY/CHLO layer by layer thin films (b) on Quartz slides.

Compared to P3TAA thin film, energy band gap of PPY thin film does not show a lot different in measurement after CHLO thin film is deposited on top of it. The value reduces to 5.8 eV from 6.0 eV when there is no CHLO thin film deposition, as shown in Figure 4.2 (a) and (b).



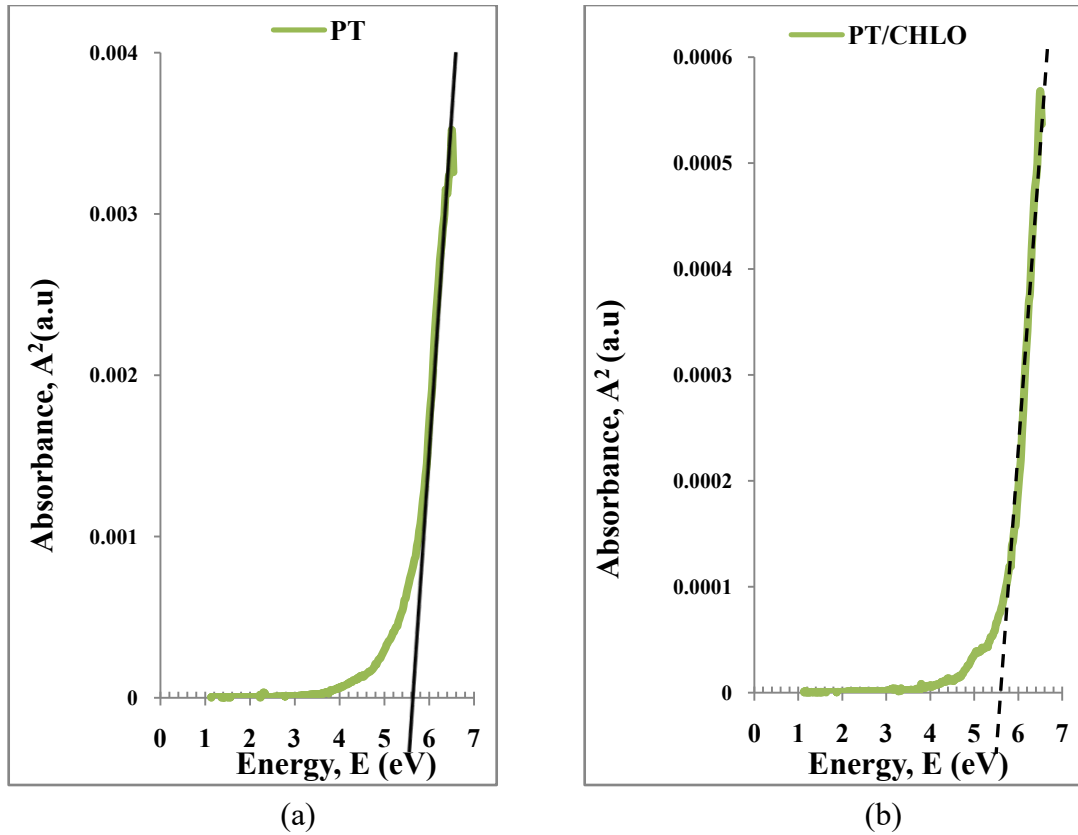


Figure 4.3: Energy band gap of PT single layer thin film (a) and energy band gap of PT/CHLO layer by layer thin films (b) on Quartz slides.

There is only a slight difference in energy band gap of PT thin film before and after CHLO thin film is deposited on top of it. Starting at around 5.7 eV as shown in Figure 4.3 (a), it reduces to 5.6 eV with the existence of CHLO thin film, as the one shows in Figure 4.3 (b). Compared to other polymers thin film, PT has the smallest difference in energy band gap before and after CHLO thin film is deposited.

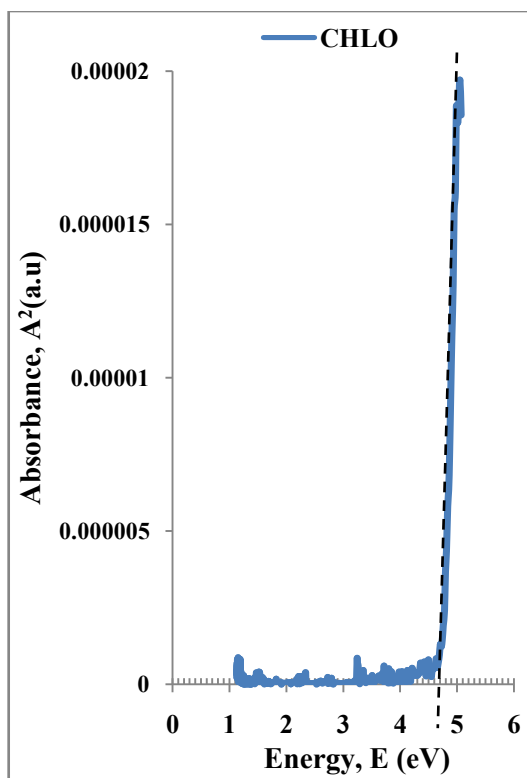


Figure 4.4: Energy band gap of single layer CHLO thin film deposited on Quartz slide.

The energy band gap of single layer CHLO thin film is 4.7 eV, as shown in Figure 4.4 much lower compared to other single layer polymer thin films. Not like other materials, CHLO which has two main types; CHLO a and CHLO b, has a behavior that can absorb energy in a wide range of spectrum. CHLO a and CHLO b can strongly absorb red part and blue part of the spectrum respectively. With the existence of CHLO thin film on top of polymer thin film, more photons can be absorbed and electrons can gain enough energy to jump from highest occupied molecular orbital (HOMO) to lowest unoccupied molecular orbital (LUMO).

Among all polymer thin films, P3TAA has the lowest energy band gap. This might be due to the addition of alkyl substituent in the third position of the aromatic ring. This modification is commonly used by other researchers (Bakhshi & Balla, 2004; Hou *et al.*,

2008) to decrease band gap, increasing polarizabilities and conductivity. By altering polymer ring with sidegroup substitution will increase the conjugation length thus elevating HOMO level of polymers. As HOMO level elevating closer to LUMO level, the gap between these levels reduces.

The reduction in energy band gap occurs after coating CHLO layer on conjugated polymer films. This could be attributed to the changes in HOMO and LUMO levels between those two materials. As HOMO level in CHLO film stating higher than HOMO level in polymer film and LUMO level in CHLO stating lower than LUMO level in polymer, the separation between HOMO level of polymer and LUMO level of CHLO is reduced. This reduction gives electron a requirement of much less energy to be excited from HOMO to LUMO and the ability to absorb light at longer wavelength. The absorption of light at longer wavelength will shrink the energy band gap.

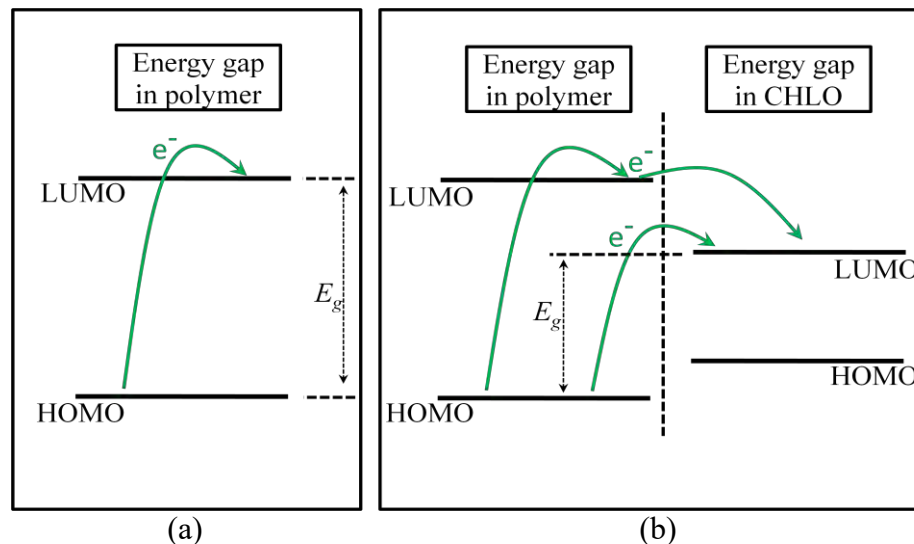


Figure 4.5: Illustration of energy required by electron to be excited from HOMO to LUMO level before coating CHLO layer (a) and after coating CHLO layer (b).

Figure 4.5 shows the illustration of energy required by an electron to be excited from HOMO to LUMO level before and after coating with CHLO layer. In previous photovoltaic experiments, Segui *et al.* (1991) and Tugulea & Antohe (1992) have used the same method by sandwiching chlorophyll between two electrodes to enhance the performance of large-band gap semiconductor in absorbing maximum photon.

### 4.3 Electrical Conductivity Measurement

Figure 4.6 shows the electrical conductivity of single layer thin films under different light intensities.

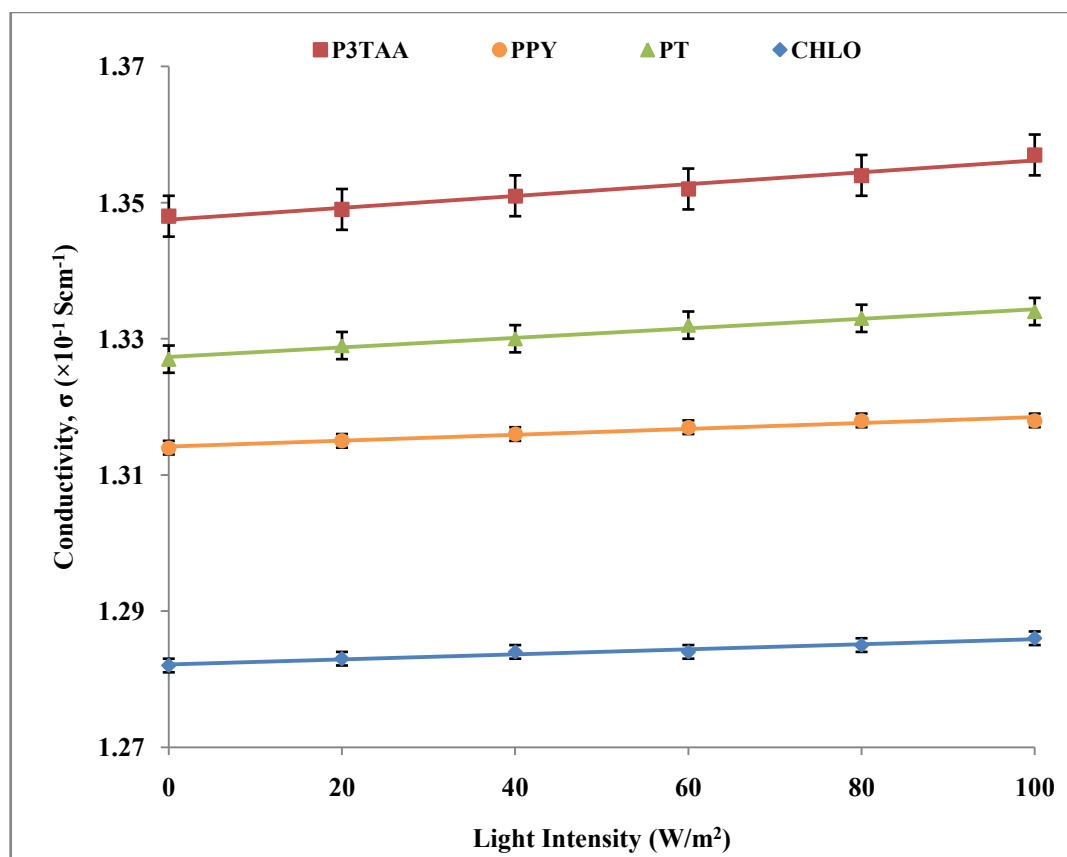


Figure 4.6: The dependence of electrical conductivity on light intensity of single layer thin films deposited on ITO coated substrates.

From Figure 4.6, as light intensity increases the electrical conductivity slightly increasing. This case is the same as reported by Hasiah *et al.* (2008). Under dark condition or in other word, even without gaining energy from photon absorption, these single layer thin films can conduct electricity. This is because conjugated polymers have alternating double and single bond and this provides a pathway for delocalized  $\pi$  electrons. The applied electric field creates a path for electrons to be hopped between polymer intrachains where the movement of electrons produces electricity. These polymers which have a delocalized  $\pi$  electron system can also absorb photons and create photogenerated charge carriers and transport these carriers even though in small amounts (Serap *et al.*, 2007). The other reason is due to the difference work function; around 0.5 eV to 0.6 eV, between ITO electrode (4.8 eV – 4.9 eV) and aluminium (Al) electrode (4.3 eV). It is also reported by Parker (1994) and Kevin & Michael (2004) that in order to generate built-in electric field within a film under dark condition, it is required to sandwich the polymer between electrodes with varying work functions.

Conductivity of P3TAA thin film is higher than other thin films in range of  $1.348 \times 10^{-1} \text{ Scm}^{-1}$  to  $1.357 \times 10^{-1} \text{ Scm}^{-1}$ . This followed by PT thin film ( $1.327 \times 10^{-1} \text{ Scm}^{-1}$  to  $1.334 \times 10^{-1} \text{ Scm}^{-1}$ ) and PPY thin film with conductivity  $1.314 \times 10^{-1} \text{ Scm}^{-1}$  at  $0 \text{ Wm}^{-2}$  intensity and slightly increasing up to  $1.318 \times 10^{-1} \text{ Scm}^{-1}$  at  $100 \text{ Wm}^{-2}$  intensity. The lowest variation of conductivity for CHLO thin film is in range of  $1.282 \times 10^{-1} \text{ Scm}^{-1}$  to  $1.286 \times 10^{-1} \text{ Scm}^{-1}$ . This is believed due to more photons are projected at higher intensity thus increasing the possibility for polymers to absorb them. A large amount of photogenerated carriers able to boost up electrical conductivity as more delocalized  $\pi$  electrons movement occur.

The addition of CHLO layer on top of polymer thin films enhances the electrical conductivity of ITO/polymer thin film. This observation is shown in Figure 4.7. Conductivity of PT/CHLO thin film has slightly increased between  $1.335 \times 10^{-1} \text{ Scm}^{-1}$  to  $1.343 \times 10^{-1} \text{ Scm}^{-1}$  and PPY/CHLO thin film increased ranging from  $1.339 \times 10^{-1} \text{ Scm}^{-1}$  to  $1.344 \times 10^{-1} \text{ Scm}^{-1}$ . The CHLO layer deposition on top of P3TAA thin film drastically enhances the conductivity of P3TAA/CHLO thin film with variation from  $1.399 \times 10^{-1} \text{ Scm}^{-1}$  to  $1.404 \times 10^{-1} \text{ Scm}^{-1}$ .

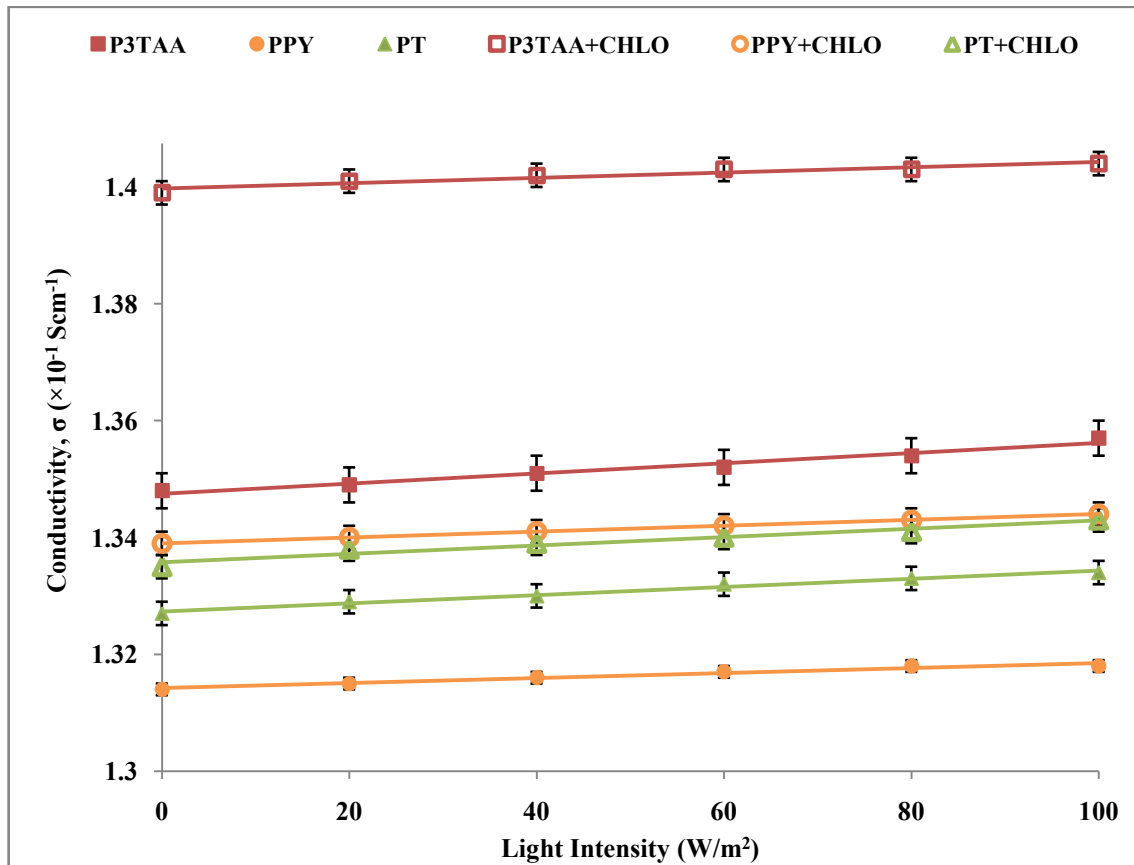


Figure 4.7: Comparison of electrical conductivity polymers thin film before and after CHLO thin film deposition.

Due to P3TAA film thickness which is thicker compared to other conjugated polymer films has given the film the possibility to absorb more projected photons. Furthermore its low energy band gap has given an extra advantage to excite more electrons from HOMO level to LUMO level thus reducing the resistivity of film. Drastic enhancement of P3TAA electrical conductivity as shown in Figure 4.7 might be due to the reduction energy band gap of P3TAA film after coating with CHLO layer. This reduction increases the number of electrons excited from HOMO to LUMO thus leading to the increasing of conductivity.

#### **4.4 Hall Effect Measurement**

Results for Hall voltage, Hall coefficient, carrier concentration, Hall mobility are shown in Figure 4.8 to Figure 4.11 respectively. It is noted that heterocyclic conjugated polymers (PT and PPY) differ significantly in their environmental stability. In neutral state, PT is stable at ambient conditions. However PPY is extremely reactive and even with minute amounts of oxygen affects its reaction (Adam & Patrice, 2007).

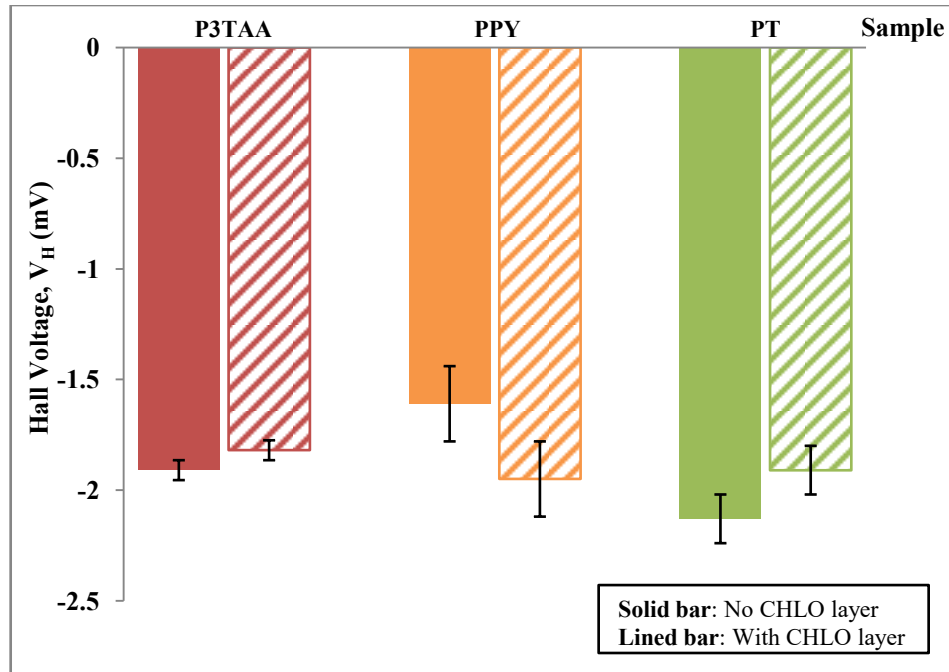


Figure 4.8: Hall voltage of organic solar cells without and with the existence of CHLO thin film at 1 Tesla applied magnetic field.

As shown in Figure 4.8, Hall voltages of devices decrease with the addition of CHLO layer except for PPY polymer device increases from -1.61 mV to -1.95 mV. With a difference of 0.9 mV, Hall voltage for P3TAA cell decreases from -1.91 mV to -1.82 mV and PT polymer cell decreases from -2.13 mV to -1.91 mV with 0.12 mV after depositing CHLO layer on top of polymer thin film.



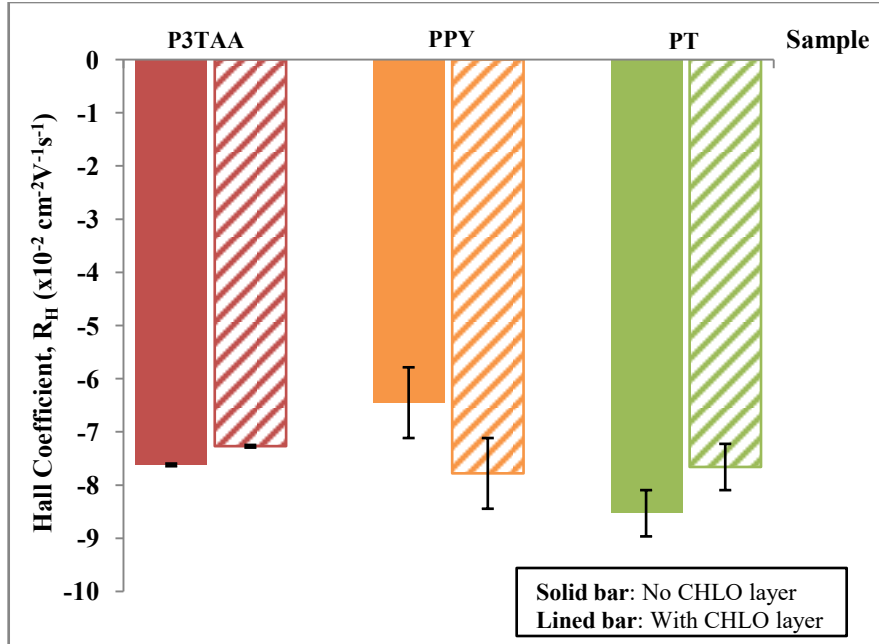


Figure 4.9: Hall coefficient of organic solar cells without and with CHLO thin film deposition at 1 Tesla applied magnetic field.

The changes in Hall coefficient with the existence of CHLO layer is the same as in Hall voltage and is shown in Figure 4.9. The cell with P3TAA polymer and PT polymer cell have decreased from  $-7.62 \times 10^{-2} \text{ cm}^{-2} \text{ V}^{-1} \text{ s}^{-1}$  to  $-7.67 \times 10^{-2} \text{ cm}^{-2} \text{ V}^{-1} \text{ s}^{-1}$  and from  $-8.53 \times 10^{-2} \text{ cm}^{-2} \text{ V}^{-1} \text{ s}^{-1}$  to  $-7.66 \times 10^{-2} \text{ cm}^{-2} \text{ V}^{-1} \text{ s}^{-1}$  respectively. Except for PPY polymer cell, Hall coefficient increases from  $-6.45 \times 10^{-2} \text{ cm}^{-2} \text{ V}^{-1} \text{ s}^{-1}$  to  $-7.78 \times 10^{-2} \text{ cm}^{-2} \text{ V}^{-1} \text{ s}^{-1}$ . Both Hall voltage and Hall coefficient are in negative field show that the majority charges in devices is electrons. If the majority of charges in device is holes, value for Hall voltage and Hall coefficient are in positive field.

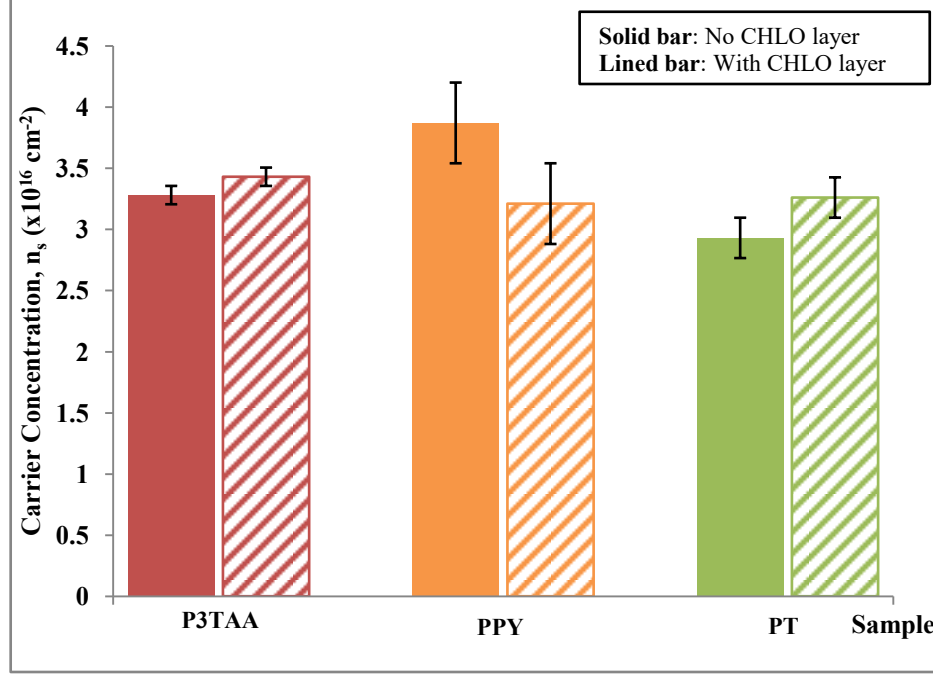


Figure 4.10: Carrier concentration of organic solar cells without and with CHLO thin film deposition at 1 Tesla applied magnetic field.

Device with PPY polymer thin film has a huge gap in carrier concentration after depositing CHLO layer compared to others. The value decreases from  $3.87 \times 10^{16} \text{ cm}^{-2}$  to  $3.21 \times 10^{16} \text{ cm}^{-2}$ . The carrier concentration for other devices slightly increases after CHLO layer deposition. The value for P3TAA device increases from  $3.28 \times 10^{16} \text{ cm}^{-2}$  to  $3.43 \times 10^{16} \text{ cm}^{-2}$  and for PT device, the carrier concentration increases from  $2.93 \times 10^{16} \text{ cm}^{-2}$  to  $3.26 \times 10^{16} \text{ cm}^{-2}$ . By comparing Figure 4.8 to Figure 4.10, relationship between Hall voltage and carrier concentration follow the illustration of Equation 4.8 below.

$$V_H = \left( \frac{1}{nq} \right) \left( \frac{I_x B_z}{t} \right) \quad (4.8)$$

Hall voltage  $V_H$ , depends on carrier concentration of sample. The increasing of carrier concentration,  $n$  and film thickness,  $t$  of sample contributes to the decreasing of the Hall voltage. In other word, Hall voltage is reciprocal to the carrier concentration.

As stated in Benramache *et al.* (2013) report, the increasing of electrical conductivity increases carrier concentration. The ability of CHLO in absorbing a wide range of spectrum increases the amount of photons absorbed thus leading to a conductivity enhancement as more photogenerated carriers are created. This causing the concentration of carriers increases as illustrated by P3TAA and PT films in Figure 4.10. However PPY situation differs theoretically. This could be attributed to the non-uniformity of film distribution during polymerization and the small numbers of polymer islands formation. Lowest in thickness gives PPY a disadvantage to absorb more photons as light projected toward cell by assuming formation of polymer islands are spreading apart (according to the value of PPY thickness standard deviation). Distribution of CHLO layer on top of PPY film by filling up the gap between boundaries might be a consequence to the carrier concentration decreasing.

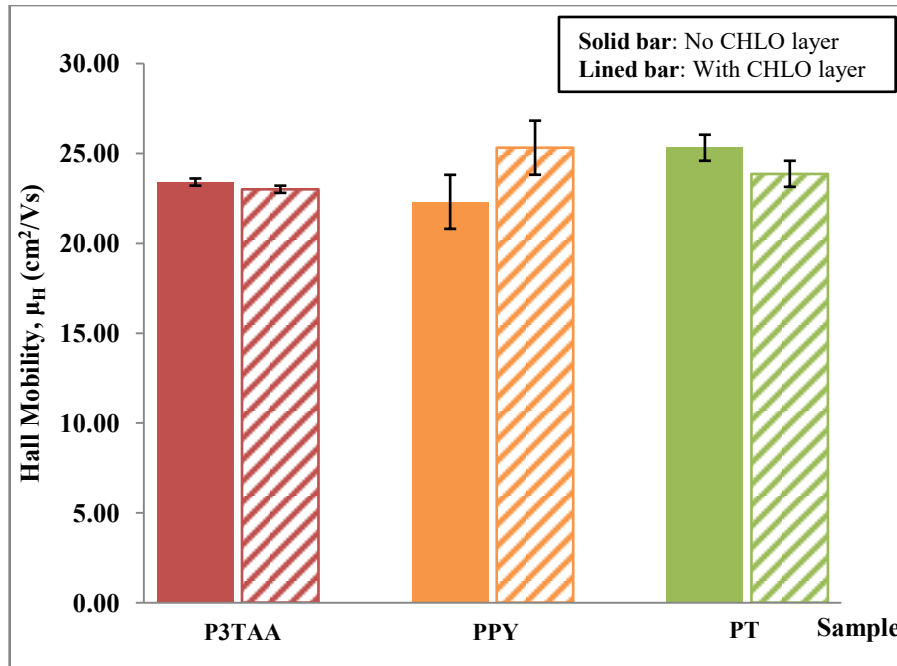


Figure 4.11: Hall mobility of organic solar cells without and with the existence of CHLO thin film at 1 Tesla applied magnetic field.

As shown in Figure 4.11, the Hall mobility ( $\mu_H$ ) of device with polymer P3TAA, PPY and PT before CHLO layer deposition is  $23.40 \text{ cm}^2/\text{Vs}$ ,  $22.30 \text{ cm}^2/\text{Vs}$  and  $25.31 \text{ cm}^2/\text{Vs}$  respectively. After CHLO layer is deposited on top of each device, Hall mobility of P3TAA sample and PT sample slightly decreases to  $23.00 \text{ cm}^2/\text{Vs}$  and  $23.86 \text{ cm}^2/\text{Vs}$  respectively but PPY sample increases to  $25.31 \text{ cm}^2/\text{Vs}$ . It is well known that there are many factors affecting organic solar cell efficiency including charge carrier mobility. Padinger *et al.* on 2003 has once reported that low charge mobility inside the photoactive matrix of polymer solar cells is one of the factors limiting the devices' efficiency. Higher mobility means higher conductivity which then lead to a better device performance. However the decreasing of Hall mobility in P3TAA and PT device with addition of CHLO layer deposition in Figure 4.11 does not equivalent to the increasing of electrical conductivity in both devices as shown in Figure 4.7.

As what have been mentioned before, the non-uniformity of polymer film deposition on ITO glass substrate where formation of polymer islands with a gap between island boundaries might be a factor causing a drop in electrical conductivity thus lowering charge mobility. As this gap growing bigger, this limits the ability of charge carriers to hop from one molecule to other molecule freely and delay the time taken for a whole charge transport process to occur.

Type of charge carriers can be verified by the polarity of Hall voltage and Hall coefficient. By referring Figure 4.8 and Figure 4.9, polarity of both Hall voltage and Hall coefficient are negative. Hence the type of major charge carriers in all these devices is electrons or to be said an *n*-type device. Polythiophene, P3TAA and PPY are all conjugated polymers and they possess conjugated  $\pi$  electrons which mean electrons are delocalized rather than being part of one valence bond. In that case these devices performance significantly depend on the power conversion efficiency with which charge carriers (electrons or holes) move within the  $\pi$ -conjugated materials (Coropceanu *et al.*, 2007).

#### **4.5 Power Conversion Efficiency**

Figure 4.12 shows three stages of organic solar cell, starting with ITO substrate without any deposition, followed by ITO substrate with polymer and CHLO deposition and a complete organic solar cell with Aluminium electrode deposition on top.

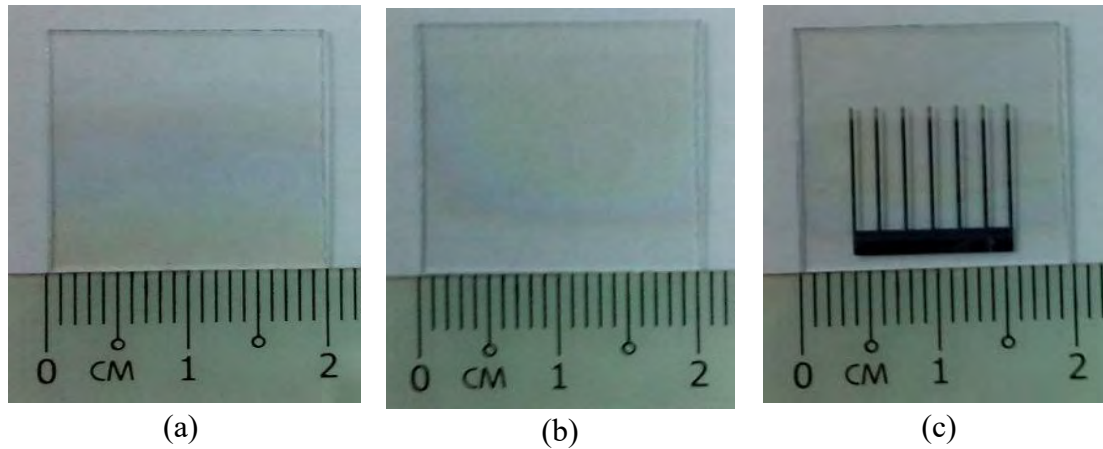


Figure 4.12: ITO substrate without any deposition (a), ITO substrate with polymer and CHLO deposition (b) and complete organic solar cell with Aluminium electrode deposition (c).

The J-V curve of organic solar cell in dark condition and under illumination  $100 \text{ W/m}^2$  at room temperature is shown in Figure 4.13. In dark condition, open circuit voltage  $V_{OC}$  and short circuit current  $I_{SC}$  crosses at 0 values. The J-V curve does not cross through fourth quadrant. Under illumination the curve shifts down to negative currents entering fourth quadrant. The device parameters can be determined and calculated in this area as shown in Figure 2.4 in Chapter 2 and by using Equation 2.3 and 2.4. Photon absorption does not occur in dark condition, so the energy supply comes from outside of device that is via the applied voltage. Under illumination, photons are absorbed into the device, so the energy supply occurs inside the cell through photogeneration of electron-hole pairs.

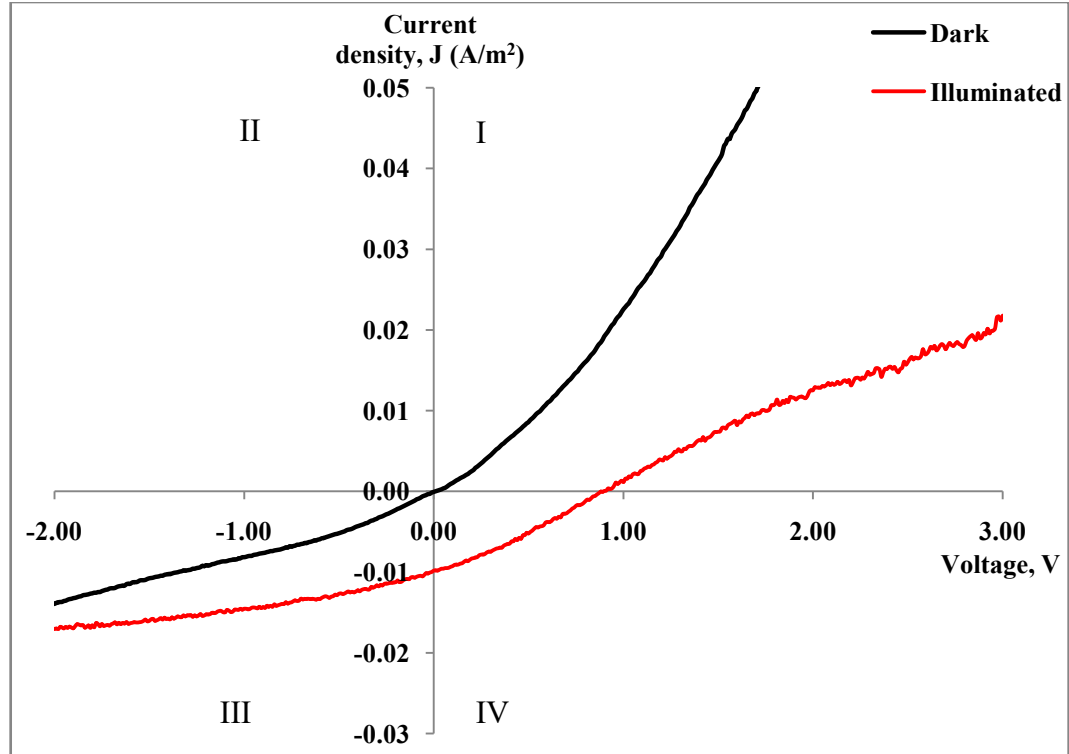


Figure 4.13: J-V characteristic of organic solar cell in dark and under illuminate condition.

Table 4.2: Efficiency and other parameters for all devices before and after depositing CHLO thin film under  $100 \text{ W/m}^2$  intensity.

Device	$V_{oc}$ ( $\times 10^{-2}$ V)	$I_{sc}$ ( $\times 10^{-7}$ A)	$P_m$ ( $\times 10^{-7}$ W)	FF ( $\times 10^{-2}$ )	PCE ( $\times 10^{-2}$ ) (%)
CHLO	93.3 ( $\pm 58.8$ )	35.0 ( $\pm 0.8$ )	10.6 ( $\pm 7.5$ )	31.8 ( $\pm 5.6$ )	2.7 ( $\pm 1.9$ )
P3TAA	34.8 ( $\pm 1.1$ )	40.2 ( $\pm 0.3$ )	4.1 ( $\pm 0.5$ )	28.5 ( $\pm 2.9$ )	1.1 ( $\pm 0.1$ )
P3TAA/CHLO	88.9 ( $\pm 7.1$ )	40.7 ( $\pm 1.3$ )	10.4 ( $\pm 0.9$ )	28.8 ( $\pm 0.3$ )	2.6 ( $\pm 0.2$ )
PPY	63.7 ( $\pm 41.1$ )	42.9 ( $\pm 0.7$ )	8.7 ( $\pm 7.1$ )	29.7 ( $\pm 6.1$ )	2.2 ( $\pm 1.7$ )
PPY/CHLO	109.8 ( $\pm 35.1$ )	39.3 ( $\pm 0.1$ )	14.9 ( $\pm 4.7$ )	34.7 ( $\pm 4.9$ )	3.7 ( $\pm 1.2$ )
PT	18.2 ( $\pm 1.6$ )	42.3 ( $\pm 0.4$ )	2.1 ( $\pm 0.2$ )	27.9 ( $\pm 0.7$ )	0.5 ( $\pm 0.1$ )
PT/CHLO	95.2 ( $\pm 3.1$ )	42.9 ( $\pm 0.5$ )	12.4 ( $\pm 1.1$ )	30.6 ( $\pm 3.6$ )	3.1 ( $\pm 0.3$ )

Table 4.2 shows important devices parameters that affect power conversion efficiency (PCE). All parameters are determined from I-V characteristic of each device under illumination of  $100 \text{ W/m}^2$ . Maximum power  $P_m$  is calculated by multiplying maximum current  $I_m$  to maximum voltage  $V_m$  gathered in fourth quadrant of I-V curve. Fill factor (FF) determines the quality of the curve and it depends on the ratio between  $I_{SC}$ ,  $V_{OC}$  and  $I_m$ ,  $V_m$ . Device with PPY/CHLO has the highest PCE with  $3.7 \times 10^{-2}\%$  compared to others. Power conversion efficiency of single layer CHLO device itself is quite high with  $2.7 \times 10^{-2}\%$  and the addition of deposited CHLO thin film on top of polymer devices has slightly increase the reading of other parameters including PCE. These parameters can vary the curvature of J-V characteristic in fourth quadrant from convex (FF > 50%) to concave (FF < 12.5%).

From Zhang *et al.* on 2011, when the device contact is perfect Ohmic contact it is believed that the difference in potential between LUMO of acceptor and HUMO of donor affects  $V_{OC}$ . The difference of PT device efficiency before and after CHLO layer deposition is the highest where it increases from  $0.5 \times 10^{-2}\%$  to  $3.1 \times 10^{-2}\%$ . Due to poor charge carrier generation and unstable charge transport, power conversion efficiency of a single layer photovoltaic cell is very low (Wöhrle & Meissner, 1991).

The responsible of chlorophyll for both light absorption and light induced charge separation have increased the PCE especially when chlorophyll is adsorbed on nanostructured semiconductor electrodes as reported by Kay & Gratzel (1993) and Bedja *et al.* (1996). For a clearer version, PCE for all devices under illumination  $100 \text{ W/m}^2$  is plotted in bar graph as shown in Figure 4.14.



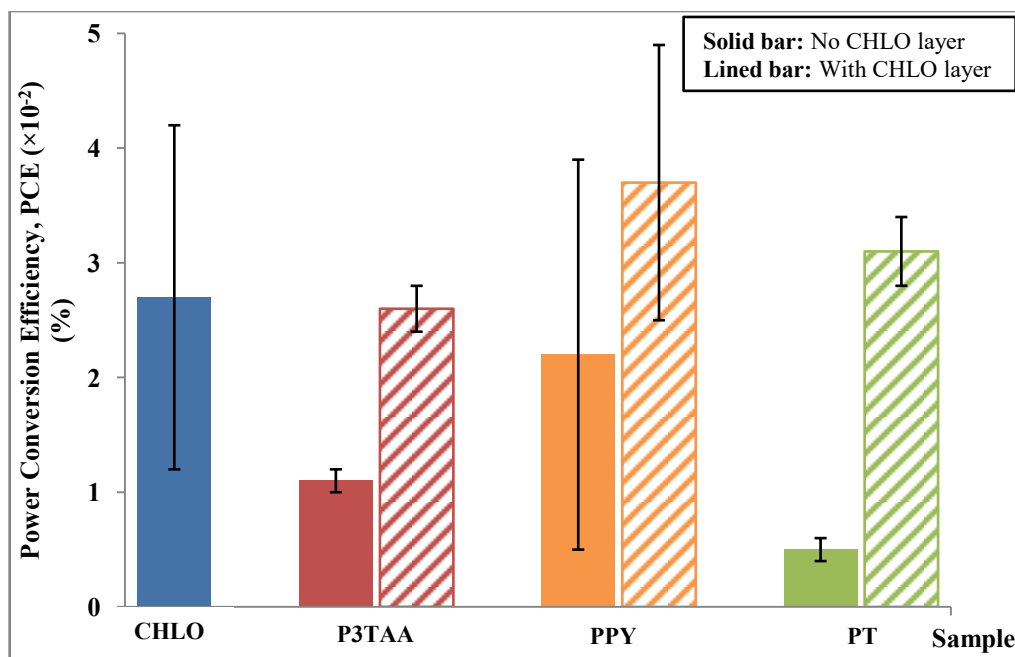


Figure 4.14: Efficiency (in percentage) of organic solar cells before (solid bar) and after deposited with CHLO thin film (lined bar) at intensity  $100 \text{ W/m}^2$ .

Table 4.3: Percentage difference of efficiency values of organic solar cells before and after CHLO thin film deposition at various light intensities.

Sample	Light intensity (W/m <sup>2</sup> )	PCE( $\times 10^{-2}$ ) (%)		Percentage difference (%)
		No CHLO layer	With CHLO layer	
P3TAA	10	1.1	2.6	1.6
PPY		2.9	1.9	0.3
PT		1.1	1.8	0.7
P3TAA	30	0.2	10.4	43.4
PPY		2.1	2.2	0.1
PT		1.6	2.5	0.6
P3TAA	60	0.6	1.7	1.8
PPY		3.8	2.2	0.4
PT		0.6	2.2	2.8
P3TAA	100	1.1	2.6	1.6
PPY		2.2	3.7	0.7
PT		0.5	3.1	4.8

Table 4.3 shows PCE of all devices under various light intensities, starting from 10 W/m<sup>2</sup> to 100 W/m<sup>2</sup> together with percentage difference of PCE before and after CHLO thin film deposition. Power conversion efficiency of devices almost gradually increases with the increasing of light intensity. The dependence of PCE onto light intensity has also been reported by Youngju *et al.* (2011) and Irene *et al.* (2011). Overall, P3TAA device shows a major percentage difference compared to others, particularly at intensity 30 W/m<sup>2</sup> with 43.4%. As what can be seen in Figure 4.14, PPY device shows a higher PCE at 100 W/m<sup>2</sup> but in general the percentage difference of the efficiency is much lower than others. The electrical properties of P3TAA show a drastic change with the existence of CHLO thin film on top of cell followed by PT and PPY device.

Conjugated polymers deposition led to large band gap semiconductors. The deposition of CHLO layer that acts as electron acceptor (electron-transfer agent) allows high excitons dissociation at donor-acceptor interface, thus preventing direct recombination and allowing electrons and holes transfer toward their derivative electrodes. Other than Hasiah *et al.* (2008), Wang *et al.* (2013a) has also reported in the increasing of PCE devices as a consequence of CHLO film deposition as acceptor layer.

## CHAPTER 5

### GENERAL DISCUSSION

This chapter discusses knowledge related to this study. Explanations on results previewed are also discussed in detail for a better understanding.

#### 5.1 Discussion

Single layer thin films on ITO substrate and the second layer, CHLO thin film on top of conjugated polymers thin film were successfully deposited using EIS and spin coater respectively. The fact that thin films were able to be deposited using these methods could be an alternative option to fabricate organic solar cells at large scale as fabrication cost in total is low. By using profilometer, the measured thickness of single layer P3TAA thin film with 97.03 nm was the highest and nearest to the optimal thickness (100 nm) in order to absorb maximum light. All thin films did not distributed uniformly on ITO substrate due to formation of small nodules at early stage of deposition which grew to form islands. These island formation and their boundaries contribute to different reading at each point taken on each film surface. Types of material used play a major role in structuring film thickness since the same method, the parameter set and the same solvent were used to deposit these films.

Among all single layer thin films deposited on Quartz, CHLO thin film has the lowest energy band gap that is 4.8 eV. However among single layer conjugated polymers, P3TAA thin film has the lowest energy band gap with 5.6 eV. Due to improved crystallinity as film thickness increasing, the UV absorption edge shifts to longer wavelength thus lowering the energy band gap. Furthermore the substitution of alkyl group in the third position of aromatic ring, as of P3TAA polymer, decrease energy band gap as a significant to the increasing of conjugation length and elevating HOMO level of polymers. By coating polymer film with spin coated CHLO layer has further decreased the energy band gap. The changes of HOMO and LUMO layer between polymer and CHLO layer might be a contribution factor. As HOMO level of CHLO layer stating higher than HOMO layer of polymer, the gap of energy between HOMO level for polymer and LUMO level for CHLO layer was narrowed.

Even under dark condition, these conjugated polymer thin films were found to able to conduct electric. This is due to the alternating single and double bond which provide a pathway and ability for  $\pi$ -electron to delocalize between bonded carbons with the application of electric field. Various incident light intensities did affect electrical conductivity of polymer thin films, CHLO thin film and combination of both. The conductivity slightly increased with the increasing of intensity as a consequence of more photons absorbed and more electron movements. After depositing CHLO as a coated layer on top of polymer films, electrical conductivity showed an improvement which was attributed to the efficient ability of chlorophyll in absorbing light. Moreover particle sizes in thin films are related to film conductivity. Particle sizes increase with the increasing of film thickness since particle boundaries in a given area decreases. The

growth of grain sizes from small nodules to islands formation lower the intergrain electron hopping lead to the enhancement of conductivity.

Data for Hall voltage, Hall coefficient, carrier concentration and Hall mobility for polymer thin film without and with coated CHLO layer were measured and collected by using HEM. The polarity sign of  $V_{H\,avg}$  and  $R_{H\,avg}$  obtained from HEM were negative for all cells. This indicates that the majority charge carriers are electron. The carrier concentration in P3TAA and PT devices slightly increased with the addition of CHLO layer but decreased in PPY device. The increasing concentration might attribute to the ability of CHLO in absorbing light. As photogenerated carriers increased, electrical conductivity increased thus increasing carrier concentration. And the decreasing value might be caused of carrier recombination and grain boundaries. Hall mobility of devices influences the efficiency. A better device performance meaning that the conductivity and carrier mobility are both high. However, unlike PPY device, Hall mobility of P3TAA and PT devices decreased after coating with CHLO layer and did not equivalent to the increasing conductivity results collected. Due to the gap between island boundaries that formed during polymerization has limited the ability of charge carriers to hop from one molecule to other molecule freely and delay the time taken for a whole charge transport process to occur thus decreasing the carrier mobility.

Power conversion efficiency (PCE) for all devices (single and double layer) was calculated under different light intensities. All device parameters including  $I_m$ ,  $V_m$ ,  $P_m$ ,  $V_{OC}$ ,  $I_{SC}$  and FF affected device's performance. Intensity of light used affected these parameters since they are dependent on each other in determining the efficiency of

devices. The PCE of single layer devices were lower compared to devices coated with CHLO layer. Since all process starting from photons absorption, excitons formation, exciton diffusion and charge carrier transportation occur in the same single layer, the optimum device performance is limited by charge recombination, poor charge carrier generation and unstable charge transport. A maximum light absorption strictly depends on film thickness and type of material used in active layer deposition. Optimal thickness (~100 nm) is required for conjugated polymer film to absorb a maximum of light.

With the addition of CHLO layer on top of polymer film, PCE of all devices slightly increased. As a consequence of the efficient ability of chlorophyll in absorbing light more photons absorption occur and reduced the possibility for free charge carrier to recombine during distributed to the associate electrodes. In general, P3TAA device has the highest percentage difference of PCE before and after depositing CHLO layer. The addition of alkyl group substituent in the third position of the aromatic ring has increased the conjugation length, decreasing band gap, increasing conductivity and promoting a better device performance.

Overall, all these polymers shows potential to be used as an active layer in fabricating organic solar cell since they are able to conduct electricity. However film deposition must reach an optimum thickness with a better surface morphology so a maximum light absorption and a higher electrical conductivity can occur. Even single layer organic solar cells generally have lower efficiency which cannot be fabricated for a large scale in meeting the marketing demands, the effectiveness of material characteristics can be well studied and understood for future needs. By adding an efficient light absorbing

material layer, as CHLO it can promote a better device performance. This shows that with a better modification, an optimum organic solar cell performance is possible to be fabricated in large scale while meeting the needs of marketing demands.

Organic solar cell with higher power conversion efficiency is a main goal to be achieved in order to substitute inorganic solar cell as a main source of sustainable energy. However, organic solar cell architecture alteration is a must to produce the best device performance especially those three conjugated polymers (P3TAA, PPY and PT) are in consideration to be used as an active layer. Film thickness can be controlled during fabrication by using more suitable method. Even if the same method is used (electrochemical method) other solution condition can be applied. This includes stirring the solution during film deposition or increasing the temperature of polymer solution for a better film deposition. Besides, different types of solvent can be used to synthesis conjugated polymers since type of solvent used can affect thickness and surface morphology of deposited thin film.

By controlling the thickness and surface morphology, the film can be more uniformly distributed. Annealing process can be done after film deposition. Annealed polymer films at suitable temperature can increase the crystallinity of film. This can contribute to a shorter path for electrons transmission since grain sizes increase which reduces grain boundaries. As more electrons are transmitted a higher efficiency can be achieved due to less possibility of free charges recombination.

The characteristic of conjugated polymers can be adjusted for a better light absorption material, a better carrier transition medium and a better insulator. This can be done by

differentiating alkyl group substituent in the third position of aromatic ring. Dopants can also be introduced to conjugated polymer. Backbone polymer adjustment and doping process can be used as an alternative to decrease energy band gap and altering the HOMO level of polymer. Small band gap conjugated polymer is a solid promise in producing organic solar cell with higher efficiency. With less energy requirement for electrons to be excited from HOMO level to LUMO level, more electrons can be dissociated and distributed to required electrode.

Instead of coating device with CHLO layer, both materials can be mixed up to fabricate a bulk heterojunction organic solar cell. Bulk heterojunction is believed to be more efficient than just heterojunction cell due to optimal film thickness can be accomplished. At optimal thickness, electrons transmission pathway are shorter and more electrons are able to be collected at desired electrode within their lifetime. Besides, other type of materials with more efficient ability can be replaced with chlorophyll to be used as coating layer if bilayer solar cell is in consideration. A small band gap organic material can be an option in order to maximize the number of electrons to be excited to LUMO level. This can decrease the possibility of free charges recombination thus transporting more electrons and holes toward appropriate electrodes.



## CHAPTER 6

### CONCLUSION AND RECOMMENDATION

This chapter concludes that results and data analyses of this study. There are also few recommendations for future research on this scope of study is presented so that better results would be achieved and a further research could be done under different parameters for a better understanding on structure of organic solar cells.

#### 6.1 Conclusion

All thin films were successfully deposited on ITO substrate by using EIS and spin coater with their thickness measured range from 50.5nm to 97.1nm but thin films did not distribute uniformly.

Energy gap of P3TAA, PPY and PT was 5.6eV, 6.0eV and 5.7eV respectively and decreased to 4.8eV, 5.8eV and 5.6eV respectively after depositing with CHLO thin film.

Majority charge carries in all OSCs were electrons and the addition of CHLO layer has increased these electrons and enhanced the electrical conductivity thus increasing the PCE of cells.

Device performances were enhanced after depositing CHLO layer on top of polymer thin films.

## **5.2 Recommendation**

More suitable thin film fabrication method can be used in order to improve surface morphology either by stirring the solution throughout EIS process or by increasing the temperature of polymer solution. Method with controllable film thickness is also recommended so an optimum film thickness can be produced.

Process of doping and adjusting polymer backbone can be introduced to increase the conjugation length of polymer thus lowering the energy band gap. More photon can be generated and more electrons can be excited from HOMO to LUMO.

Mixing two materials with efficient ability in light absorption is also recommended. Bulk heterojunction organic solar cell is believed to be more efficient in absorbing light and diffusing electrons toward anode since electrons transmission pathway are shorten.

The knowledge in conjugated polymer characteristic such as P3TAA, PPY and PT need to be narrowly studied and understood due to their possibility as inorganic solar cell substituent. Therefore, these findings may provide impressing information for future research which brings to the new prospective in organic optoelectronic applications.

## REFERENCES

- Abdelaziz, E., Saidur, R. & Mekhilef, S. (2011). A review on energy saving strategies in industrial sector. *Renewable Sustainable Energy Reviews*, 15(1), 150-168.
- Adam, P. & Patrice, R. (2002). Processible conjugated polymers: from organic semiconductors to organic metals and superconductors. *Progress in Polymer Science*, 27, 135-190.
- Antoniadis, H., Hsieh, B.R., Abkowitz, M. A., Jenekhe, S. A. & Stolka, M. (1994). Photovoltaic and photoconductive properties of aluminum/poly(p-phenylene vinylene) interfaces. *Synthetic Metals*, 62, 265-271.
- Apaydin, D. H., Yildiz, D. E., Cirpana, A. & Toppare, L. (2013). Optimizing the organic solar cell efficiency: Role of the active layer thickness. *Solar Energy Materials & Solar Cells*, 113, 100-105.
- Bakhshi, A. K. & Bhalla, G. (2004). Electrically conducting polymers: Materials of the twentyfirst century. *Journal of Scientific & Industrial Research*, 63, 715-728.
- Banos, R., Manzano-Agugliaro, F., Montoya, F., Gil, C., Alcayde, A. & Gomez, J. (2011). Optimization methods applied to renewable and sustainable energy: A review. *Renewable Sustainable Energy Reviews*, 15, 1753-1766.
- Bedja, I., Kamat, P. V. & Hotchandani, S. (1996). Fluorescence and photoelectrochemical behavior of chlorophyll a adsorbed on a nanocrystalline SnO<sub>2</sub> film. *Journal of Applied Physics*, 80, 4637-4643.
- Benramache, S., Belahssen, O., Guettaf, A. & Arif, A. (2013). Correlation between electrical conductivity–optical band gap energy and precursor molarities ultrasonic spray deposition of ZnO thin films. *Journal of Semiconductors*, 34, 11.
- Borrelli, D. C., Barr, M. C., Bulovic, V. K. & Gleason, K. (2012). Bilayer heterojunction polymer solar cells using unsubstituted polythiophene via oxidative chemical vapor deposition. *Solar Energy Materials & Solar Cells*, 99, 190-196.
- Boudouris, B. W. (2009). Polythiophene-containing block copolymers for organic photovoltaic applications. Ph.D Thesis, University of Minnesota, Minnesota.

- Brabec, C. J., Sariciftci, N. S. & Hummelen, J. C. (2001). Plastic solar cells. *Advanced Functional Materials*, 11, 15-26.
- Chainet, E. and Billon, M. (1998). In situ study of polypyrrole morphology by STM: effect of the doping state. *Journal of Electroanalytical Chemistry*, 451, 273-277.
- Chamberlain, G. A. (1983). Organic solar cells: A review. *Solar Cells*, 8, 47.
- Charters, W. W. (2001). Developing markets for renewable energy technologies. *Renewable Energy*, 22, 217-222.
- Chen, X. (2007). Synthesis and characterization of Polythiophene and derivatives. Thesis for PhD, The University of Texas, Arlington, United State of America.
- Coakley, K. M., Liu, Y. X., McGehee, M. D., Frindell, K. L. & Stucky, G. D. (2003). Infiltrating semiconducting polymers into self-assembled mesoporous titaniafilms for photovoltaic applications. *Advanced Functional Materials*, 13, 301-306.
- Coropceanu, V., Cornil, J., da Silva Filho, D. A., Olivier, Y., Silbey, R. & Brédas, J. L. (2007). Charge transport in organic semiconductors. *Chemical Reviews*, 107, 926-952.
- de Boer, R.W.I., Gershenson, M.E., Morpurgo, A.F. & Podzorov, V. (2004). Organic single-crystal field-effect transistor. *Physica Status Solidi A*, 201(6), 1302-1331.
- Demirbas, A. (2000). Recent advances in biomass conversion technologies. *Energy Education Science and Technology*, 6, 19-40.
- Dimitrakopoulos, C. D. & Malenfant, P. R. L. (2002). Organic thin film transistors for large area electronics. *Advanced Materials*, 14, 99-117.
- Dincer, I. (1999). Environmental impacts of energy. *Energy Policy*, 27, 845-854.
- Farchioni, R. & Grosso, G. (2001). Organic Electronic Materials (Ed). Springer, Berlin.
- Giglioti, M., Trivinho-Strixino, F., Matsushima, J. T., Bulhões, L. O. S. & Pereira, E. C. (2004). Electrochemical and electrochromic response of poly(thiophene-3-acetic acid) films. *Solar Energy Materials & Solar Cells*, 82, 413-420.

- Goh, C., Scully, S. R. & McGehee, M. D. (2007). Effects of molecular interface modification in hybrid organic-inorganic photovoltaic cells. *Journal of Applied Physics*, 101(11), 114503 1-12.
- Grossiord, N., Kroon, J. M., Andriessen, R. & Blom, P. W. M. (2012). Degradation mechanisms in organic photovoltaic devices. *Organic Electronics*, 13, 432–456.
- Guo, X., Martin, B. & Müllen, K. (2013). Designing conjugated polymers for organic electronics. *Progress in Polymer Science*, 38, 1832-1908.
- Gupta, D., Mukhopadhyay, S. & Narayan, K. S. (2010). Fill factor in organic solar cells. *Solar Energy Materials and Solar Cells*, 94, 1309-1313.
- Gupta, S. K., Sharma, A., Banerjee, S., Gahlot, R., Aggarwal, N., Deepaka & Garga, A. (2013). Understanding the role of thickness and morphology of the constituent layers on the performance of inverted organic solar cells. *Solar Energy Materials & Solar Cells*, 116, 135-143.
- Hagen, K. (2006). Organic electronics: Materials, manufacturing, and applications (Ed). Weinheim, Germany: Wiley-VCH Verlag GmbH & Co. KGaA.
- Halls, J. J. M., Pichler, K., Friend, R. H., Moratti, S. C. & Holmes, A. B. (1996). Exciton diffusion and dissociation in a poly(*p*-phenylenevinylene)/C60 heterojunction photovoltaic cell. *Applied Physics Letters*, 68, 3120.
- Hara, K., Horiguchi, T., Kinoshita, T., Sayama, K., Sugihara, H. & Arakawa, H. (2000). Highly efficient photon-to-electron conversion with mercurochrome-sensitized nanoporous oxide semiconductor solar cells. *Solar Energy Materials and Solar Cells*, 64, 115.
- Hara, K., Sayama, K., Arakawa, H., Ohga, Y., Shinpo, A. & Suga, S. (2001a). A coumarine-derivative dye sensitised nanocrystalline TiO<sub>2</sub> solar cell having a high solar-energy conversion efficiency up to 5.6%. *Chemical Communications*, 569-570.
- Hara, K., Sugihara, H., Tachibana, Y., Islam, A., Yanagida, M., Sayama, K., Arakawa, H., Fujihashi, G., Horiguchi, T. & Kinoshita, T. (2001b). Dye-sensitized nanocrystalline TiO<sub>2</sub> solar cells based on ruthenium (II) phenanthroline complex photosensitizers. *Langmuir*, 17(19), 5992-5999.

- Hasiah, S. & Senin, H. B. (2007). Electrical characterization of chlorophyll. *Journal of Sustainability Science and Management*, 2(1), 95-98.
- Hasiah, S., Ibrahim, K., Senin, H. B. & Halim, K. B. K. (2008). Electrical conductivity of chlorophyll with polythiophene thin film on indium tin oxide as p-n heterojunction solar cell. *Journal of Physical Science*, 19(2), 77-92.
- Haugeneder, A., Neges, M., Kallinger, C., Spirkl, W., Lemmer, U., Feldmann, J., Scherf, U., Harth, E., Gügel, A. & Müllen, K. (1999). Exciton diffusion and dissociation in conjugated polymer/fullerene blends and heterostructures. *Physical Review B*, 59, 15346.
- Haeldermans, I., Truijen, I., Vandewal, K., Moons, W., Van Bael, M. K., D'Haen, J., Manca, J. V. & Mullens, J. (2008). Water based preparation method for „green“ solid-state polythiophene solar cells. *Thin Solid Films*, 516, 7245–7250.
- Hoppe, H. & Sariciftci, N. S. (2008). Polymer solar cells. *Advances in Polymer Science*, 214, 1-86.
- Hossein, E. (2007). Studying the characteristics of polypyrrole and its composites. *World Journal of Chemistry* 2, 2, 67-74.
- Hou, J. H., Park, M. H., Zhang, S. Q, Yao, Y., Chen, L. M., Li, J. H. & Yang, Y. (2008). Bandgap and molecular energy level control of conjugated polymer photovoltaic materials based on benzo[1,2-b:4,5-b']dithiophene. *Macromolecules*, 41, 6012-6018.
- Hwang, J., Wan, A. & Kahn, A. (2009). Energetics of metal-organic interfaces: New experiments and assessment of the field. *Materials Science and Engineering Reports*, 64, 1-31.
- Irene, G. V., Youhai, Y., Belén, B., Judith, O. & Monica, L. C. (2011). Synthesis conditions, light intensity and temperature effect on the performance of ZnO nanorods-based dye sensitized solar cells. *Journal of Power Sources*, 196, 6609-6621.
- Janssen, R. (2005). Introduction to polymer solar cells - (3Y280). Departments of Chemical Engineering & Chemistry and Applied Physics Eindhoven University of Technology, The Netherlands.

- Kalogirou, S. (2004). Solar thermal collectors and applications. *Progress in Energy and Combustion Science*, 30, 231-295.
- Kashiyama, Y., Yokoyama, A., Shiratori, T., Inouye, I., Kinoshita, Y., Mizoguchi, T. & Tamiaki, H. (2013).  $^{13}\text{C}$ ,  $^{17}\text{O}$ -Cyclophosphoramide b enol as a catabolite of chlorophyll b in phycophagy by protists. *FEBS Letters*, 587, 2578–2583.
- Kaur, N., Singh, M., Dinesh, P., Tomas, W. & Nunzi, J.M. (2014). Organic materials for photovoltaic applications: Review and mechanism. *Synthetic Metals*, 190, 20-26.
- Kay, A. & Gratzel, M. (1993). Photosensitization of  $\text{TiO}_2$  solar cells with chlorophyll derivatives and related natural porphyrins. Artificial Photosynthesis 1, *Journal of Physical Chemistry*, 97, 6272-6277.
- Kevin, M. C. & Michael, D. M. (2004). Conjugated polymer photovoltaic cells. *Chemistry of Materials*, 16, 4533-4542.
- Khairul, W. M., Fairuz, M. Y., Rafizah, R., Adibah, I. D., Maryam, S. J., Faizuddin, M. A. H., Hasyah, S., Hasyiya, K. A. & Meng, G. T. (2013). Single molecule thin film featuring disubstituted thiourea (TU) doped with chlorophyll as potential active layer in photovoltaic cell. *International Journal of Electrochemical Science*, 8, 8175-8190.
- Kim, M. S. (2009). Understanding organic photovoltaic cells: Electrode, nanostructure, reliability and performance. Thesis for PhD, The University of Michigan, USA.
- Kim, Y. G., Walker, J., Samuelson, L. A. & Kumar, J. (2003). Efficient light harvesting polymers for nanocrystalline  $\text{TiO}_2$  photovoltaic cells. *Nano Letters*, 3, 523.
- Lenzen, M. (2010). Current state of development of electricity-generating technologies: A literature review. *Energies*, 3, 462-591.
- Li, W. T., Tsao, H. W., Chen, Y. Y., Cheng, S. W. & Hsu, Y. C. (2007). A study on the photodynamic properties of chlorophyll derivatives using human hepatocellular carcinoma cells. *Photochemical and Photobiological Sciences*, 6, 1341-1348.
- Liu, L. M. & Liu, G. M. (2011). Investigation of recombination loss in organic solar cells by simulating intensity-dependent current–voltage measurements. *Solar Energy Materials & Solar Cells*, 95, 2557-2563.

- Liu, Y., Scully, S. R., McGehee, M. D., Liu, J., Luscombe, C. K., Fréchet, J. M. J., Shaheen, S. E. & Ginley, D. S. (2006). Dependence of band offset and open circuit voltage on the interfacial interaction between TiO<sub>2</sub> and carboxylated polythiophenes. *Journal of Physical Chemistry B*, 110(7), 3257-3261.
- Loudon, M. G. (2002). Chemistry of naphthalene and the aromatic heterocycles. *Organic Chemistry* (4th ed.). New York: Oxford University Press. pp. 1135-1136
- Luzzati, S., Basso, M., Catellani, M., Brabec, C. J., Gebeyehu, D. & Sariciftci, N. S. (2002). Photo-induced electron transfer from a dithieno thiophene-based polymer to TiO<sub>2</sub>. *Thin Solid Films*, 403, 52.
- Manzano-Agugliaro, F. (2010). Use of bovine manure for ex situ bioremediation of diesel contaminated soils in Mexico. *Technical Information Economica Agraria*, 106(3), 197-207.
- Manzano-Agugliaro, F., Alcayde, A., Montoya, F., Zapata-Sierra, A. & Gil, C. (2013). Scientific production of renewable energies worldwide: An overview. *Renewable Sustainable Energy Reviews*, 18, 134-143.
- Manzano-Agugliaro, F., Sanchez-Muros, M. J., Barroso, F. G., Martínez-Sánchez, A., Rojo, S. & Pérez-Bañón, C. (2012). Insects for biodiesel production. *Renewable Sustainable Energy Reviews*, 16, 3744-3753.
- Marks, R. N., Halls, J. J. M., Bradley, D. D. C., Friend, R. H. & Holmes, A. B. (1994). The photovoltaic response in poly(p-phenylene vinylene) thin-film devices. *Journal of Physics: Condensed Matter*, 6, 1379.
- Mihailetchi, V. D., Koster, L. J. A. & Blom, P. W. M. (2004). Effect of metal electrodes on the performance of polymer:fullerene bulk heterojunction solar cells. *Applied Physics Letters*, 85, 970-972.
- Miller-Chou, B. A. & Koenig, J. L. (2003). A review of polymer dissolution. *Progress in Polymer Science*, 28, 1223-1270.
- Mishra, A. & Buerle, P. (2012). Small molecule organic semiconductors on the move: Promises for future solar energy technology. *Angewandte Chemie International Edition*, 51, 2020-2067.



- Newman, C. R., Frisbie, C. D. da Silva Filho, D. A., Brédas, J. L., Ewbank, P. C. & Mann, K. R. (2004). Introduction to organic thin film transistors and design of n-channel organic semiconductors. *Chemistry of Materials*, 16, 4436-4451.
- Ogi T., Modesto-Lopez L. B., Iskandar F. & Okuyuma, K. (2007). Fabrication of a large area monolayer of silica particles on a sapphire substrate by a spin coating method. *Colloids and Surfaces A: Physicochemical and Engineering Aspects*, 297, 71.
- Padinger, F., Rittberger, R. S. & Sariciftci, N. S. (2013). Effect of postproduction treatment on plastic solar cell. *Advanced Functional Materials*, 2(13), 1-4.
- Pagliaro, M., Ciriminna, R. & Palmisano, G. (2008). Flexible solar cell. *ChemSusChem*, 1, 880.
- Panwar, N., Kaushik, S. & Kothari, S. (2011). Role of renewable energy sources in environmental protection: a review. *Renewable Sustainable Energy Reviews*, 15, 1513-1524.
- Parker, I. D. (1994). Carrier tunneling and device characteristics in polymer light-emitting diodes. *Journal of Applied Physics*, 75, 1656.
- Pettersson, L. A. A., Roman, L. S. & Inganäs, O. (1999). Modeling photocurrent action spectra of photovoltaic devices based on organic thin films. *Journal of Applied Physics*, 86, 487.
- Rafizah R., Khairul, W. M., Hasiyah, S., Hasyiya, K. A., Isa, M. I. N. & Meng, G. T. (2013). Synthesis, characterization and electrochemical analysis of v-shaped disubstituted thiourea-chlorophyll thin film as active layer in organic solar cell. *International Journal of Electrochemical Science*, 8, 3333-3348.
- Rieß, W., Karg, S., Dyakonov, V., Meier, M. & Schworer, M. (1994). Electroluminescence and photovoltaic effect in PPV Schottky diodes. *Journal of Luminescence*, 60-61, 906-911.
- Roncali, J. (1997). Synthetic principles for bandgap control in linear ir-conjugated systems. *Chemical Reviews*, 97, 173-205.
- Rostalski, J. & Meissner, D. (2000). Monochromatic versus solar efficiencies of organic solar cells. *Solar Energy Materials & Solar Cells*, 61, 87-95.

- Savanije, T. J., Warman, J. M. & Goossens, A. (1998). Visible light sensitisation of titanium dioxide using a phenylene vinylene polymer. *Chemical Physics Letters*, 287, 148.
- Segui, J., Hotchandani, S., Baddou, D. & Leblanc, R. M. (1991). Photoelectric properties of ITO/CdS/Chlorophyll a/Ag heterojunction solar cells. *Journal of Physical Chemistry*, 95, 8807-8812.
- Serap, G., Helmut, N., & Niyazi, S. S. (2007). Conjugated polymer-based organic solar cells. *Chemical Reviews*, 107, 1324-1338.
- Shinde, S. S., Park, S. & Shin, J. (2015). Spin synthesis of monolayer of SiO<sub>2</sub> thin films. *Journal of Semiconductors*, 36(4), 1-10.
- Steima, R., Ameri, T., Schilinsky, P., Waldauf, C., Dennler, G, Scharber, M. & Brabec, C. J. (2011). Organic photovoltaics for low light applications. *Solar Energy Materials & Solar Cells*, 95, 3256-3261.
- Stoessel, M., Wittmann, G., Staudigel, J., Steuber, F., Blässing, J., Roth, W., Klausmann, H., Rogler, W., Simmerer, J., Winnacker, A., Inbasekaran, M. & Woo, E. P. (2000). Cathodeinduced luminescence quenching in polyfluorenes. *Journal of Applied Physics*, 87, 4467.
- Sun, L. & Wang, S. (2004). Spectral and nonlinear optical properties of chlorophyll b depends on distortion of two-dimensional electron configuration along one axis. *Dyes and Pigments*, 61, 273–278.
- Sun, S. & Sariciftci, N. S. (2005). Organic photovoltaics: Mechanisms, materials, and devices (eds). Boca Raton, Florida: Taylor & Francis.
- Tamiaki, H., Shibata, R. & Mizoguchi, T. (2007). The 17-propionate function of (bacterio)chlorophylls: Biological implication of their long esterifying chains in photosynthetic systems. *Photochemical and Photobiology*, 83, 152-162.
- Tang, C. W. (1986). Two-layer organic photovoltaic cell. *Applied Physics Letters*, 48, 183-185.
- Tang, Q., Jiang, L., Tong, Y., Li, H., Liu, Y., Wang, Z., Hu, W., Liu, Y. & Zhu, D. (2008). Micrometer and nanometer sized organic single-crystalline transistors. *Advanced Materials*, 20, 2947-2951.

- Treiber, A., Dansette, P. M., Amri, H. E., Girault, J. P., Ginderow, D., Mornon, J. P. & Mansuy, D. (1997). Chemical and biological oxidation of thiophene: Preparation and complete characterization of thiophene *s*-oxide dimers and evidence for thiophene *s*-oxide as an intermediate in thiophene metabolism in vivo and in vitro. *Journal of American Chemical Society*, *119*(7), 1565-1571.
- Tsuchiya, T., Shikida, M. & Sato, K. (2002). Tensile testing system for sub-micrometer thick films. *Sensors and Actuators A*, *97-98*, 492-496.
- Tugulea, L. & Antohe, S. (1992). Photovoltaic characteristics of Si/Chlorophyll a structure, in N.Murata (ed.). *Research in Photosynthesis*, *Kluwer Academic Publishers*, *11*, 845-848.
- Valls, I. G., Yu, Y. H., Ballesteros, B., Oro, J. & Cantu, M. L. (2011). Synthesis conditions, light intensity and temperature effect on the performance of ZnO nanorods-based dye sensitized solar cells. *Journal of Power Sources*, *196*, 6609-6621.
- Viau, L., Hihn, J. Y., Lakard, S., Moutarlier, V., Flaud, V. & Lakard, B. (2014). Full characterization of polypyrrole thin films electrosynthesized in room temperature ionic liquids, water or acetonitrile. *Electrochimica Acta*, *137*, 298-310.
- Wang, X. F. & Tamiaki, H. (2010). Cyclic tetrapyrrole based molecules for dye-sensitized solar cells. *Energy Environment of Science*, *3*, 94-106.
- Wang, X. F., Tamiaki, H., Kitao, O., Ikeuchi, T. & Sasaki, S. I. (2013a). Molecular engineering on a chlorophyll derivative, chlorin  $e_6$ , for significantly improved power conversion efficiency in dye-sensitized solar cells. *Journal of Power Sources*, *242*, 860-864.
- Wang, Y. W., Sasaki, S. I., Zhuang, T., Tamiaki, H., Zhang, J. P., Ikeuchi, T., Hong, Z., Kido, J. & Wang, X. F. (2013b). Dicyano-functionalized chlorophyll derivatives with ambipolar characteristic for organic photovoltaics. *Organic Electronics*, *14*, 1972-1979.
- Wehenkel, D. J., Hendriks, K. H., Wienk, M. M. & Janssen, A. J. (2012). The effect of bias light on the spectral reponsivity of organic solar cells. *Organic Electronics*, *13*, 3284-3290.

- William, B. (2005). Introduction to conjugated polymers. In *Electronics and optical properties of conjugated polymers*, pp 1, New York: Oxford University Press.
- Wöhrle, D. & Meissner, D. (1991). Organic solar cells. *Advanced Material*, 3, 129-138.
- Wusheng, Yin, Li, J., Li, Y. M., Wu, J. P. & Gu, T. (2001). Conducting composite film based on polypyrrole and crosslinked cellulose. *Journal of Applied Polymer Science*, 80(9), 1368-1373.
- Yanagida, S., Senadeera, G. K. R., Nakamura, K., Kitamura, T. & Wada. Y. (2004). Polythiophene-sensitized TiO<sub>2</sub> solar cells. *Journal of Photochemistry and Photobiology A: Chemistry*, 166, 75–80
- Yeh, N. & Yeh, P. (2013). Organic solar cells: Their developments and potentials. *Renewable and Sustainable Energy Reviews*, 21, 421-431.
- Yongju, P., Seunguk, N., Donggu, L., Kim, J.Y. & Changhee, L. (2011). Temperature and light intensity dependence of polymer solar cells with MoO<sub>3</sub> and PEDOT:PSS as a buffer layer. *Journal of the Korean Physical Society*, 59(2), 362-366.
- Zhang, F. J., Xu, X. W., Tang, W. H., Zhang, J., Zhuo, Z., Wang, J., Wang, J., Xu, Z. & Wang, Y. S. (2011). Recent development of the inverted configuration organic solar cells. *Solar Energy Materials & Solar Cells*, 95, 1785-1799.
- Zhang, F. J., Zhao, D. W., Zhuo, Z. L., Wang, H, Xu, Z. & Wang, Y. S. (2010). Inverted small molecule organic solar cells with Ca modified ITO as cathode and MoO<sub>3</sub> modified Ag as anode. *Solar Energy Materials & Solar Cells*, 94, 2416-2421.
- Zhang, Z. G. & Wang, J. Z. (2012). Structures and properties of conjugated Donor–Acceptor copolymers for solar cell applications. *Journal of Materials Chemistry*, 22, 4178-87.

## APENDIX A

Hall Effect Measurement readings for all devices at 1 Tesla (10kG) magnetic field application

Hall Effect Measurements	Magnetic field (kG)	Device					
		P3TAA	P3TAA + CHLO	PPY	PPY + CHLO	PT	PT + CHLO
Ohmic contact voltage, V							
V+42,13	10	1.76E-01	1.83E-01	1.26E-01	8.97E-02	2.68E-01	2.85E-01
V-42,13	10	-1.76E-01	-1.83E-01	-1.26E-01	-8.97E-02	-2.68E-01	-2.85E-01
V+31,42	10	-1.80E-01	-1.87E-01	-1.29E-01	-9.36E-02	-2.72E-01	-2.89E-01
V-31,42	10	1.80E-01	1.87E-01	1.29E-01	9.36E-02	2.72E-01	2.89E-01
V+42,13	-10	1.80E-01	1.87E-01	1.29E-01	9.36E-02	2.72E-01	2.89E-01
V-42,13	-10	-1.80E-01	-1.87E-01	-1.29E-01	-9.36E-02	-2.72E-01	-2.89E-01
V+31,42	-10	-1.76E-01	-1.83E-01	-1.26E-01	-8.97E-02	-2.68E-01	-2.85E-01
V-31,42	-10	1.76E-01	1.83E-01	1.26E-01	8.97E-02	2.68E-01	2.85E-01
Hall coefficient, $R_{\text{havg}}$ ( $\times 10^{-2} \text{ cm}^{-2} \text{ V}^{-1} \text{ s}^{-1}$ )		-7.62	-7.27	-6.45	-7.78	-8.53	-7.66
Hall mobility, $\mu_{\text{H}}$ ( $\text{cm}^2/\text{Vs}$ )		23.40	23.00	22.30	25.31	25.31	23.86
Carrier concentration, $n_s$ ( $\times 10^{16} \text{ cm}^{-2}$ )		3.28	3.43	3.87	3.21	2.93	3.26

## APENDIX B

Single layer device parameters readings determined from IV curve under different intensities

Device Parameters	Intensity (W/m <sup>2</sup> )	SAMPLE			
		P3TAA/ITO	PPY/ITO	PT/ITO	CHLO/ITO
$V_{oc}$ ( $\times 10^{-2}$ V)	10	36.2 ( $\pm$ 16.1)	76.3 ( $\pm$ 49.9)	38.1 ( $\pm$ 3.5)	7.2 ( $\pm$ 0.2)
	30	9.3 ( $\pm$ 2.8)	58.4 ( $\pm$ 23.9)	49.1 ( $\pm$ 2.1)	24.7 ( $\pm$ 3.5)
	60	25.6 ( $\pm$ 16.1)	96.5 ( $\pm$ 6.7)	17.7 ( $\pm$ 4.9)	41.4 ( $\pm$ 22.7)
	100	34.8 ( $\pm$ 1.1)	63.7 ( $\pm$ 41.1)	18.2 ( $\pm$ 1.6)	93.3 ( $\pm$ 58.8)
$I_{sc}$ ( $\times 10^{-7}$ A)	10	38.9 ( $\pm$ 1.3)	42.3 ( $\pm$ 0.4)	41.8 ( $\pm$ 0.3)	30.4 ( $\pm$ 0.2)
	30	40.8 ( $\pm$ 0.8)	42.2 ( $\pm$ 0.5)	42.7 ( $\pm$ 0.3)	31.6 ( $\pm$ 0.4)
	60	39.7 ( $\pm$ 0.5)	42.5 ( $\pm$ 0.5)	42.9 ( $\pm$ 0.6)	32.5 ( $\pm$ 0.8)
	100	40.2 ( $\pm$ 0.3)	42.9 ( $\pm$ 0.7)	42.3 ( $\pm$ 0.4)	35.0 ( $\pm$ 0.8)
$V_m$ ( $\times 10^{-2}$ V)	10	19.1 ( $\pm$ 6.7)	38.6 ( $\pm$ 24.9)	19.8 ( $\pm$ 0.9)	3.2 ( $\pm$ 0.3)
	30	4.8 ( $\pm$ 1.2)	29.7 ( $\pm$ 13.9)	24.1 ( $\pm$ 1.6)	13.1 ( $\pm$ 3.1)
	60	12.7 ( $\pm$ 7.8)	53.9 ( $\pm$ 7.7)	10.3 ( $\pm$ 2.1)	24.1 ( $\pm$ 8.9)
	100	16.5 ( $\pm$ 1.8)	33.2 ( $\pm$ 24.8)	9.9 ( $\pm$ 0.9)	48.7 ( $\pm$ 29.7)
$I_m$ ( $\times 10^{-7}$ A)	10	20.5 ( $\pm$ 1.1)	28.9 ( $\pm$ 2.7)	22.1 ( $\pm$ 2.6)	17.8 ( $\pm$ 1.2)
	30	20.2 ( $\pm$ 1.2)	26.5 ( $\pm$ 4.2)	26.2 ( $\pm$ 0.7)	18.5 ( $\pm$ 0.5)
	60	20.1 ( $\pm$ 0.7)	28.3 ( $\pm$ 3.6)	22.7 ( $\pm$ 0.9)	23.8 ( $\pm$ 2.7)
	100	24.2 ( $\pm$ 1.1)	25.1 ( $\pm$ 2.3)	21.6 ( $\pm$ 0.3)	21.1 ( $\pm$ 2.1)
$P_m$ ( $\times 10^{-7}$ W)	10	3.9 ( $\pm$ 1.4)	11.5 ( $\pm$ 8.1)	4.3 ( $\pm$ 0.5)	0.6 ( $\pm$ 0.1)
	30	1.1 ( $\pm$ 0.3)	8.3 ( $\pm$ 5.2)	6.3 ( $\pm$ 0.3)	2.4 ( $\pm$ 0.5)
	60	2.5 ( $\pm$ 1.6)	15.4 ( $\pm$ 3.9)	2.3 ( $\pm$ 0.3)	5.6 ( $\pm$ 1.6)
	100	4.1 ( $\pm$ 0.5)	8.7 ( $\pm$ 7.1)	2.1 ( $\pm$ 0.2)	10.6 ( $\pm$ 7.5)
FF ( $\times 10^{-2}$ )	10	28.6 ( $\pm$ 2.3)	34.7 ( $\pm$ 4.2)	27.8 ( $\pm$ 4.8)	26.2 ( $\pm$ 1.4)
	30	25.7 ( $\pm$ 0.5)	31.8 ( $\pm$ 6.9)	30.2 ( $\pm$ 0.2)	30.8 ( $\pm$ 3.1)
	60	25.5 ( $\pm$ 1.6)	37.3 ( $\pm$ 7.5)	31.4 ( $\pm$ 5.4)	48.7 ( $\pm$ 20.4)
	100	28.5 ( $\pm$ 2.9)	29.7 ( $\pm$ 6.1)	27.9 ( $\pm$ 0.7)	31.8 ( $\pm$ 5.6)
PCE ( $\times 10^{-2}$ )	10	1.1 ( $\pm$ 0.4)	2.9 ( $\pm$ 2.1)	1.1 ( $\pm$ 0.1)	0.13 ( $\pm$ 0.06)
	30	0.2 ( $\pm$ 0.1)	2.1 ( $\pm$ 1.3)	1.6 ( $\pm$ 0.1)	0.6 ( $\pm$ 0.1)
	60	0.6 ( $\pm$ 0.3)	3.8 ( $\pm$ 0.9)	0.6 ( $\pm$ 0.1)	1.4 ( $\pm$ 0.4)
	100	1.1 ( $\pm$ 0.1)	2.2 ( $\pm$ 1.7)	0.5 ( $\pm$ 0.1)	2.7 ( $\pm$ 1.9)

## APENDIX C

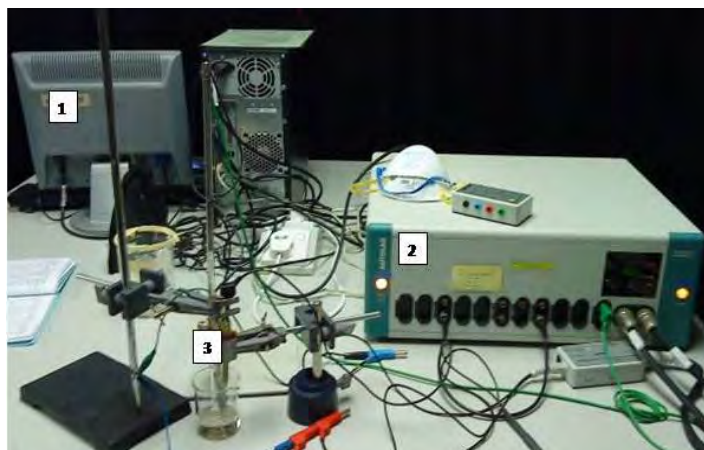
Double layer device parameters determined from IV curve under different intensities

Device Parameters	Intensity (W/m <sup>2</sup> )	SAMPLE		
		CHLO/P3TAA/ITO	CHLO/PPY/ITO	CHLO/PT/ITO
$V_{oc}$ ( $\times 10^{-2}$ V)	10	71.2 ( $\pm$ 48.2)	68.2 ( $\pm$ 4.7)	49.9 ( $\pm$ 2.8)
	30	297.7 ( $\pm$ 3.2)	72.9 ( $\pm$ 1.6)	59.2 ( $\pm$ 1.9)
	60	67.5 ( $\pm$ 4.1)	71.1 ( $\pm$ 0.2)	61.2 ( $\pm$ 15.6)
	100	88.9 ( $\pm$ 7.1)	109.8 ( $\pm$ 35.1)	95.2 ( $\pm$ 3.1)
$I_{sc}$ ( $\times 10^{-7}$ A)	10	36.9 ( $\pm$ 5.3)	37.1 ( $\pm$ 0.4)	43.2 ( $\pm$ 0.6)
	30	34.3 ( $\pm$ 1.7)	39.4 ( $\pm$ 0.3)	43.8 ( $\pm$ 0.8)
	60	39.5 ( $\pm$ 0.8)	39.8 ( $\pm$ 0.8)	43.3 ( $\pm$ 0.2)
	100	40.7 ( $\pm$ 1.3)	39.3 ( $\pm$ 0.1)	42.9 ( $\pm$ 0.5)
$V_m$ ( $\times 10^{-2}$ V)	10	40.0 ( $\pm$ 32.4)	32.9 ( $\pm$ 2.5)	28.8 ( $\pm$ 4.1)
	30	155.1 ( $\pm$ 1.7)	35.7 ( $\pm$ 0.9)	34.3 ( $\pm$ 2.1)
	60	29.2 ( $\pm$ 0.4)	34.2 ( $\pm$ 0.6)	31.7 ( $\pm$ 10.3)
	100	43.5 ( $\pm$ 41.2)	57.4 ( $\pm$ 17.7)	49.4 ( $\pm$ 3.2)
$I_m$ ( $\times 10^{-7}$ A)	10	24.4 ( $\pm$ 5.5)	23.9 ( $\pm$ 0.6)	25.3 ( $\pm$ 1.2)
	30	26.8 ( $\pm$ 1.4)	24.9 ( $\pm$ 0.6)	29.6 ( $\pm$ 2.1)
	60	24.2 ( $\pm$ 1.1)	25.9 ( $\pm$ 0.1)	26.7 ( $\pm$ 2.6)
	100	24.1 ( $\pm$ 1.8)	26.1 ( $\pm$ 1.8)	25.2 ( $\pm$ 0.7)
$P_m$ ( $\times 10^{-7}$ W)	10	10.4 ( $\pm$ 9.1)	7.8 ( $\pm$ 0.7)	7.2 ( $\pm$ 0.6)
	30	41.5 ( $\pm$ 2.1)	8.8 ( $\pm$ 0.4)	10.1 ( $\pm$ 0.2)
	60	7.1 ( $\pm$ 0.3)	8.8 ( $\pm$ 0.1)	8.6 ( $\pm$ 3.7)
	100	10.4 ( $\pm$ 0.9)	14.9 ( $\pm$ 4.7)	12.4 ( $\pm$ 1.1)
FF ( $\times 10^{-2}$ )	10	34.7 ( $\pm$ 8.1)	31.1 ( $\pm$ 1.3)	33.6 ( $\pm$ 1.1)
	30	40.6 ( $\pm$ 0.8)	30.9 ( $\pm$ 1.5)	39.1 ( $\pm$ 0.6)
	60	26.7 ( $\pm$ 0.6)	31.3 ( $\pm$ 1.1)	31.6 ( $\pm$ 5.1)
	100	28.8 ( $\pm$ 0.3)	34.7 ( $\pm$ 4.9)	30.6 ( $\pm$ 3.6)
PCE ( $\times 10^{-2}$ )	10	2.6 ( $\pm$ 2.2)	1.9 ( $\pm$ 0.2)	1.8 ( $\pm$ 0.1)
	30	10.4 ( $\pm$ 0.5)	2.2 ( $\pm$ 0.1)	2.5 ( $\pm$ 0.1)
	60	1.7 ( $\pm$ 0.1)	2.2 ( $\pm$ 0.1)	2.2 ( $\pm$ 0.9)
	100	2.6 ( $\pm$ 0.2)	3.7 ( $\pm$ 1.2)	3.1 ( $\pm$ 0.3)

## APENDIX D



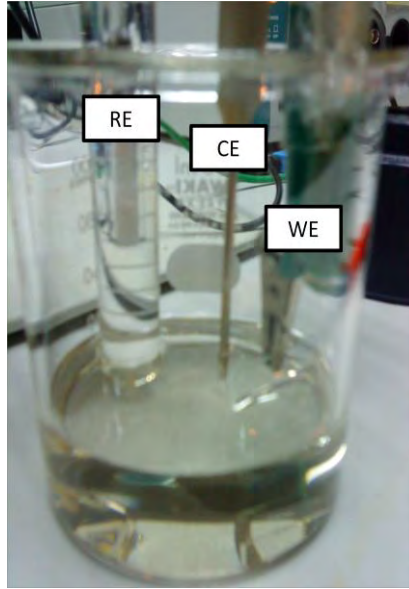
Cleaning process at room temperature using JEIOTECH US-05 Ultrasonic Cleaner (5L).



EIS experimental set-up. GPES (1), potentiostat/galvanostat (2) and electrochemical cell (3).



## APENDIX E



Thin film deposition by using EIS at room temperature under three-electrode configuration

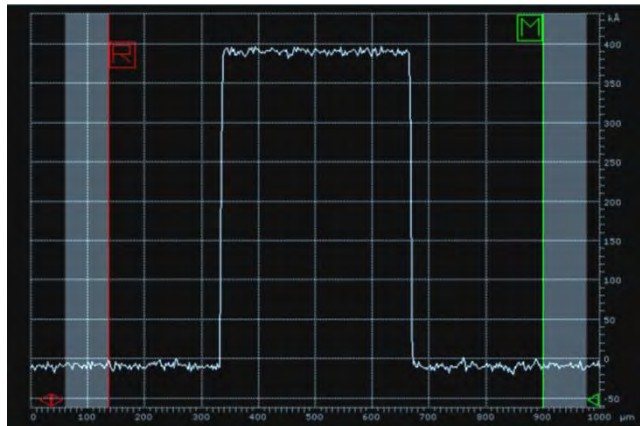


Laurell Spin Coater of model WS-400BZ-6NPP-Lite

## APENDIX F



VEECO Dektak 150 Stylus Surface Profilometer together with Detak 150 software

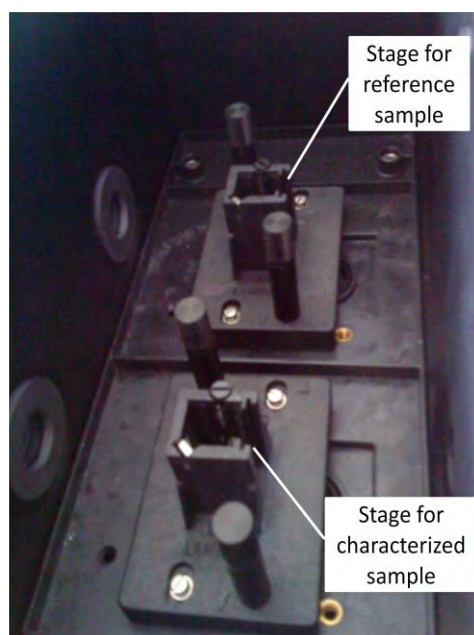


Anylizing thickness of thin film by using R-cursor and M-cursor

## APENDIX G



Perkin Elmer's instrument model Lambda 25 UV-Vis (Ultraviolet-Visible) spectrometer



Position of sample stages inside sample compartment of UV-Vis

## APENDIX H

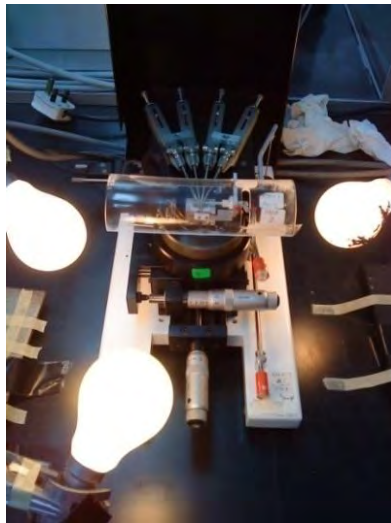


(a)



(b)

Equipments for electrical conductivity measurement, Jandel Universal Probe Station (a) and RM3000 test unit (b)



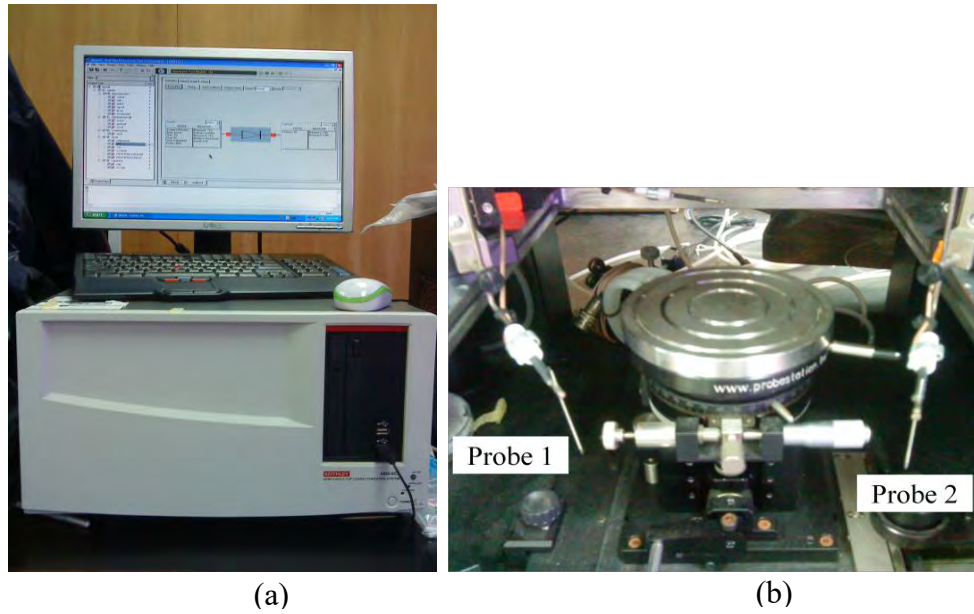
(a)



(b)

Electrical conductivity characterization under different light intensity (a) and dark condition (b)

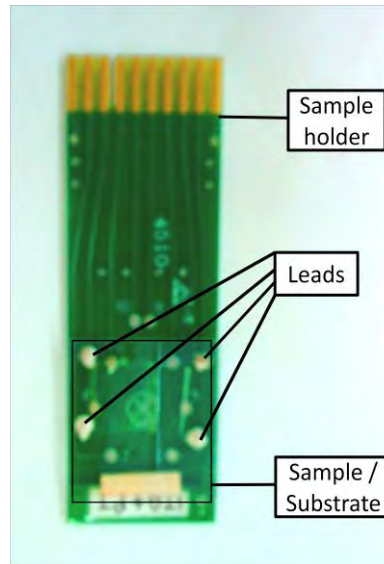
## APENDIX I



Keithley SCS's Source Measure Units connected to a computer (a) and two point probes stage station (b).



## APENDIX J



Sample holder with mounted substrate and leads

## BIODATA OF THE AUTHOR

### PERSONAL PARTICULARS

Name : Hamizah Nadia Binti Alias@Yusof  
Address : 97, Lorong Surau Baru, Pasir Panjang, 21100 Kuala Terengganu,  
Terengganu.  
Phone : 017-7738959  
Email : hamizah.alias@gmail.com  
Date of Birth : 2<sup>nd</sup> March 1988  
Citizen : Malaysian  
Race : Female  
Religion : Islam  
Education :

Master of Science (by research) Physics  
Universiti Malaysia Terengganu, (2011-2015)

Bachelor of Science in Material Physics with Second Class Honours  
Universiti Teknologi Malaysia, (2007-2010)

Pahang Matriculation College, Ministry of Education Malaysia,  
Life Sciences Matriculation, (2006-2007)

Sekolah Menengah Kebangsaan Sultan Sulaiman, Kuala Terengganu  
PMR & SPM, (2001-2005)

### PUBLICATIONS

#### Published Articles in Journal

1. S Hasiah, EAGE Ali, N Aziz, N Ali, WA Dhafina, **A Hamizah**, ARN Laily, Hazirah Che Hassan. Study the electrical properties and the efficiency of polythiophene with dye and chlorophyll as bulk hetero-junction organic solar cell. *Advanced Materials Research*, Volume 895, Pages 513-519. (May - 2014)
2. **Hamizah Nadia Bt Alias@Yusof**, Hasiah Bt Salleh, M.I.N. Isa. Polythiophene, Polypyrrole and Poly (3-thiophene acetic acid) for conjugated polymer based single layer organic solar cells. *International Journal of Applied Research and Studies* (iJARS), Volume 3, Issue 7 (July - 2014) ISSN: 2278-9480

## Proceedings

1. **A. Hamizah**, S. Hasiah, E. A. Ghapur, W. A. Dhafina & N. A. N. Aziz. Optical and electrical studies on organic solar cells. *UMT 11th International Annual Symposium on Sustainability Science and Management (UMTAS 2012)*
2. W. A. Dhafina, S. Hasiah, E. A. Ghapur, **A. Hamizah** and N. A. N. Aziz. ZnO Nanorods and P3TAA as Hybrid Solar Cells. *UMT 11<sup>th</sup> International Annual Symposium on Sustainability Science and Management (UMTAS 2012)*
3. **A. Hamizah**, S. Hasiah, E. A. Ghapur, W. A. Dhafina and N. A. N. Aziz. Conducting polymer thin film by electrochemistry method as organic solar cells. *4<sup>th</sup> International Conference on Solid State Science and Technology (4<sup>th</sup> ICSSST 2012)*
4. W.A. Dhafina, S. Hasiah, E.A. Ghapur and **A. Hamizah**. Optical and electrical properties of ZnO nanorods and P3AA thin film for use in hybrid Solar Cells. *4<sup>th</sup> International Conference on Solid State Science and Technology (4<sup>th</sup> ICSSST 2012)*
5. S. Hasiah, E.A. Ghapur, N.A.N. Aziz, W.A. Dhafina, **A. Hamizah**, A.R.N. Laily and Hazirah Che Hassan. Study the electrical properties and the efficiency of polythiophene with dye and chlorophyll as bulk heterojunction organic solar cell. *4<sup>th</sup> International Conference on Solid State Science and Technology (4<sup>th</sup> ICSSST 2012)*
6. **A. Hamizah**, S. Hasiah, E. A. Ghapur, W.A. Dhafina and N.A.N. Aziz. Efficiency Characterization on Single Layer of Polythiophene, Polypyrrole, Poly(3-Thiophene Acetic Acid) as Organic Solar Cells. *Seminar Hasil Penyelidikan Sektor Pengajian Tinggi Kementerian Pendidikan 2013 - Sains Tulin dan Gunaan (SHPKPT 2013-STG)*
7. S. Hasiah, E.A. Ghapur, N.A.N. Aziz, W.A. Dhafina and **A. Hamizah**. Etraction of chlorophyll, synthesis of polymer and growth ZnO nanoarrays for hybrid solar cell. *Seminar Hasil Penyelidikan Sektor Pengajian Tinggi Kementerian Pendidikan 2013 - Sains Tulin dan Gunaan (SHPKPT 2013-STG)*

## Submitted paper for Review

1. **Hamizah Nadia Bt Alias@Yusof**, Hasiah Bt Salleh, M.I.N. Isa. Thickness dependent on energy band gap and electrical conductivity of undoped conjugated polymer thin films. *Advanced Materials Research*. 2015.



### **Conferences Attended**

1. UMT 11<sup>th</sup> International Annual Symposium on Sustainability Science and Management (UMTAS 2012) on 9<sup>th</sup> to 11<sup>th</sup> July 2012 at Riyaz Heritage Marina & Spa, Terengganu.
2. 4<sup>th</sup> International Conference on Solid State Science and Technology (4<sup>th</sup> ICSSST 2012) on 18<sup>th</sup> to 20<sup>th</sup> December 2012 at Holiday Inn, Melaka.
3. Seminar Hasil Penyelidikan Sektor Pengajian Tinggi Kementerian Pendidikan 2013 - Sains Tulin dan Gunaan (SHPKPT 2013-STG) on 2<sup>nd</sup> and 3<sup>rd</sup> July 2013 at EDC Hotel, Universiti Utara Malaysia.